Mark Orazem and John Newman, "Photoelectrochemical Devices for Solar Energy Conversion," in Modern Aspects of Electrochemistry 18, R. E. White, J. O'M Bockris and B. E. Conway, editors, Plenum Press, New York, 1986, pp 61-112.

2

# Photoelectrochemical Devices for Solar Energy Conversion

Mark E. Orazem

*Department of Chemical Engineering, University of Virginia, Charlottesville, Virginia* 22901

John Newman

*Materials and Molecular Research Division, Lawrence Berkeley Laboratory, and Department of Chemical Engineering, University of California, Berkeley, California* 94720

Photoelectrochemical cells are distinguished by the use of a semiconductor-electrolyte interface to create the necessary junction for use as a photovoltaic device.[1-8] This chapter presents a description of this device from an electrochemical engineering viewpoint. The traditional chemical engineering fundamentals of transport phenomena, reaction kinetics, thermodynamics, and system design provide a useful foundation for the study of semiconducting devices. The motivation for the study of photoelectrochemical cells is discussed, and a physical description of the cell features is presented. A tutorial on the mechanism of cell operation is presented which includes descriptions of the phenomena of band-bending and straightening, the effect of interfacial phenomena, and current flow. Mathematical relationships are developed which describe this system, and the influence of cell design is discussed.

Many review papers, including recent chapters in this series, cover the physics and chemistry of photoelectrochemical cells (see, e.g., Refs. 9-19). The reader is referred to these for a historical

perspective of the development of the field of photoelectrochemistry as applied to photovoltaic devices. An overview of the analytic and numerical models that have been developed for photoelectrochemical cells is presented in Section III.2. This chapter is further distinguished by an emphasis on quantitative design and optimization of large-scale photoelectrochemical cells and by a mathematical description that accounts for the influence of the nonideal behavior associated with large electron and hole concentrations in the semiconductor. This review also provides a contrast between a physical description of electrons in terms of energies and statistical distributions and a chemical description in terms of concentrations and activity coefficients.

## I. SEMICONDUCTOR ELECTRODES

Semiconductors are characterized by the difference in energy between valence and conduction-band electrons. Electrons can be transferred from the valence band to the conduction band by absorption of a photon with energy greater than or equal to the transition or band-gap energy. When the electron moves into the higher energy level, it leaves behind a vacancy in the valence band, or *hole*. Both the negatively charged electrons and the positively charged holes are mobile and can serve as charge carriers (see, e.g., Refs. 20–24). In the presence of a potential gradient (or electric field), electrons and holes tend to migrate in opposite directions and can result in a net flow of electrical current. In the absence of a potential gradient, electron–hole pairs produced by illumination recombine with no net flow of electrical current. Photovoltaic devices therefore require an equilibrium potential gradient in the illuminated region of the semiconductor.

A potential gr. dient can be created by forming an interface or junction with a semiconducting material. Metal–semiconductor, $p$–$n$ semiconductor, and semiconductor–electrolyte interfaces have been used in the construction of photovoltaic cells.[25-27] The interface in a $p$–$n$ junction photovoltaic cell can be constructed by doping the surface of an $n$ or $p$-type semiconductor with atoms that invert the semiconductor type. These atoms are then thermally diffused into the host semiconductor to an optimal depth. Diffusion rates



in grain boundaries greatly exceed those in the bulk crystal; thus the need for a distinct boundary limits this technique to single-crystal host semiconductors. The junction between an electrolyte and a semiconductor, in contrast to the thermally diffused $p$–$n$ junction, is formed spontaneously when the semiconductor is immersed in the electrolyte. The doping and diffusion processes are not needed, and polycrystalline semiconductors can be used.[28] Vapor or plasma deposition of thin metallic or semiconducting films also allows construction of solar cells with polycrystalline materials. These solid-state-junction photovoltaic devices have some of the advantages attributed to photoelectrochemical cells and avoid the associated corrosion problems.[29]

### 1. Physical Description

The principal elements of the liquid-junction photovoltaic cell, as shown in Fig. 1, are the counterelectrode, the electrolyte, the semiconductor–electrolyte interface, and the semiconductor. The distribution of charged species (ionic species in the electrolyte and electrons and holes in the semiconductor) is altered by the semiconductor–electrolyte interface, and an equilibrium potential gradient is formed in the semiconductor. The interfacial region may be

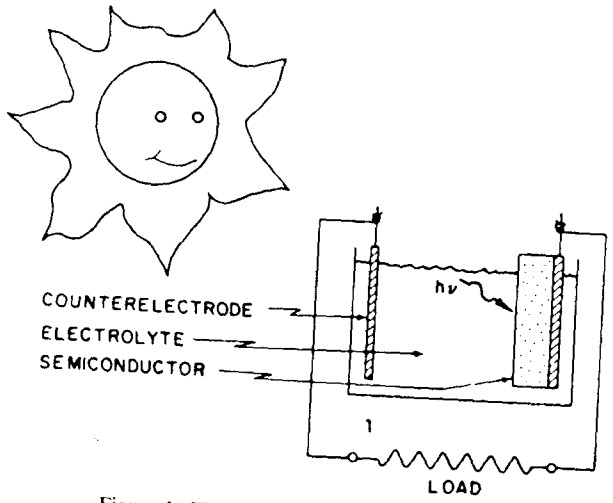


Figure 1. The photoelectrochemical cell.

associated with adsorption of charged species or with surface sites. The charge is distributed such that the interface taken as a whole is still electrically neutral. Sunlight is absorbed within the semiconductor and causes generation of electron-hole pairs which are separated by the potential gradient. This separation leads to concentration and potential driving forces for electrochemical reactions at the semiconductor-electrolyte interface. The electrochemical reactions allow passage of electrical current through the cell.

The semiconductor and the electrolyte phases are conveniently characterized through macroscopic relations. A microscopic model is required for the interface between the bulk phases. This model can be arbitrarily complex but is restricted by the requirement that thermodynamic relationships among the bulk phases hold. A convenient model for the interfacial region is represented in Fig. 2. The interface is represented by four planes, inner and outer Helmholtz planes on the electrolyte side of the interface and inner and outer surface states on the semiconductor side. The outer Helmholtz plane (OHP) is the plane of closest approach for (hydrated) ions associated with the bulk solution. The inner Helmholtz plane (IHP) passes through the center of ions specifically adsorbed on the semiconductor surface. The outer surface state (OSS) represents the plane of closest approach for electrons (and holes) associated with the bulk of the semiconductor. The inner surface state (ISS) is a plane of surface sites for adsorbed electrons. If surface sites are neglected, the ISS and the OSS are coincident.

This model of the semiconductor-electrolyte interface is an application of the classical Stern-Gouy-Chapman diffuse-double-layer theory[30-33] to the semiconductor and the electrolyte sides of the interface. Charge adsorbed onto the IHP and the ISS planes is balanced by charge in the diffuse region of the electrolyte and the space-charge region of the semiconductor. The net charge of the interface, including surface planes and diffuse and space-charge regions, is equal to zero. Within a given model, reactions may be written to relate concentrations and potentials at interfacial planes. Interfacial sites or energy levels for electrons or holes can be included at the ISS. Interfacial reactions may thus include adsorption of ionic species from the OHP to the IHP, adsorption of electrons from the OSS to sites of specified energy at the ISS, surface recombination through ISS sites, and direct surface recombination. Emission of electrons from the semiconductor may take place by electron transfer from surface sites at the ISS to adsorbed ions (trapping and subsequent emission), transfer of OSS electrons to adsorbed ions (thermionic emission), transfer of electrons in the space charge region to adsorbed ions (thermally enhanced field emission or direct tunneling), transfer of electrons in the neutral region to adsorbed ions (field emission or direct tunneling), and transfer of electrons in the neutral region to adsorbed ions through defects in the bulk (multistep tunneling). Such reactions may also involve ions associated with the OSS or with the diffuse part of the double layer. These reactions may also take place in the reverse direction. These reaction mechanisms are described by Fonash.[34]



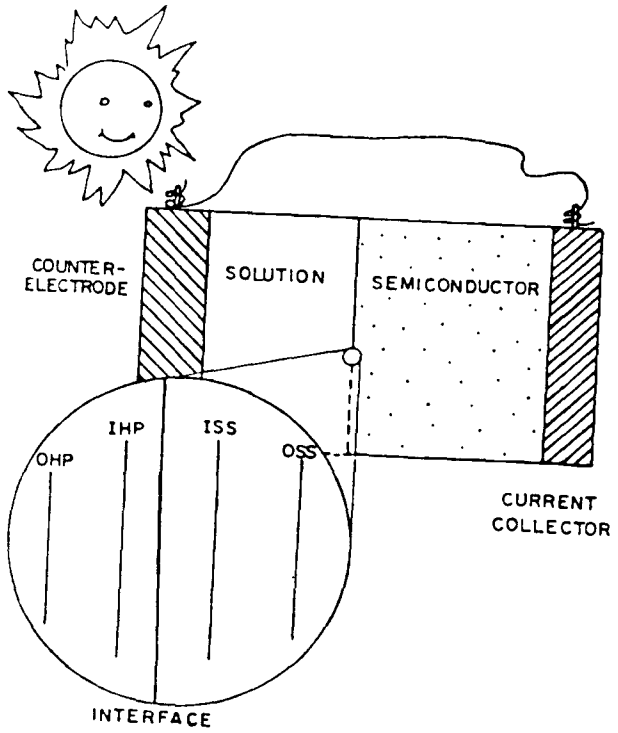


Figure 2. Physical model of the semiconductor-electrolyte interface in a photoelectrochemical cell.

## 2. The Mechanism of Cell Operation

Formation of an interface perturbs the potential distribution in the semiconductor, and this perturbation creates the junction necessary for the photovoltaic effect in solar cells. Examination of the potential distribution in the liquid-junction cell therefore provides insight into the forces driving the cell. The following discussion is based on the numerical solution of the equations governing a *n*-GaAs photoanode with a selenium redox couple (see Refs. 35-37). The governing equations are presented in Section II. Interfacial reactions were included but were assumed to be sufficiently fast that the operation of the cell was limited by the transport and generation of electrons and holes in the semiconductor. The potential distribution is presented in Fig. 3. In the dark, at open circuit (curve a), the system is equilibrated. The potential is nearly constant throughout the solution and the interfacial planes (OHP, IHP, ISS, and OSS). The potential varies in the semiconductor in response

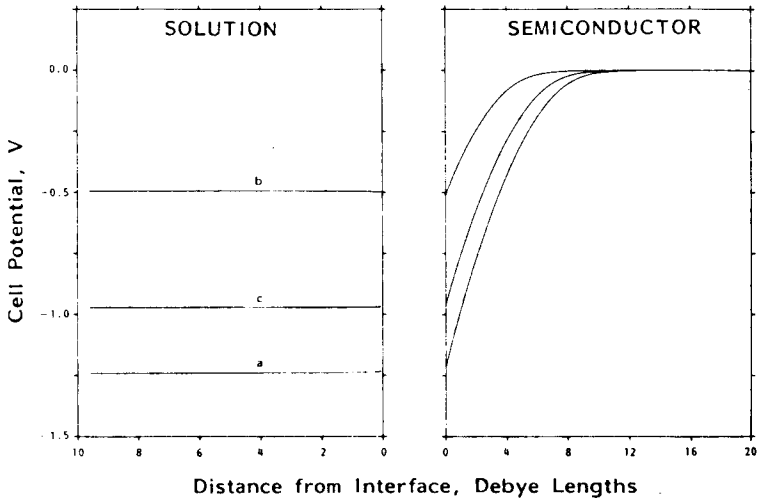


Figure 3. Potential distribution for an *n*-GaAs rotating disk electrode with no interfacial kinetic limitations. Curve a, open circuit in the dark; curve b, open circuit under 882 W/m$^2$ illumination; and curve c, near short circuit ($i = -23.1$ mA/cm$^2$) under illumination. The electrolytic Debye length is 0.2 nm, and the semiconductor Debye length is 70 nm.



to charge distributed in the semiconductor. This variation of electrical potential in the equilibrated semiconductor is termed *band-bending*. The *flat-band potential* is the potential that would need to be applied in order to achieve uniform potential in the semiconductor.

Under illumination at open circuit (curve b), the concentrations of electrons and holes increase, and the variation of potential in the semiconductor decreases. The decrease in potential variation in response to illumination is referred to as the *straightening of the bands*. The charges of holes and electrons, generated by the illumination, tend to go in opposite directions under the influence of the electric field. Their accumulation, at open circuit, at various locations creates an electric field which tends to cancel that existing in the dark and leads to this straightening of the bands. The difference between the potential in the dark and under illumination represents a driving force for flow of electrical current. The potential distribution near the short-circuit condition (curve c) approaches the equilibrium distribution. Short circuit is defined as the condition of a zero cell potential. The description presented here neglects the influence of electrolyte resistance and counterelectrode kinetic and mass-transfer limitations in determining the condition of short circuit. The inclusion of these effects cause the short-circuit potential distributions described here to occur at negative cell potentials. All the variation in potential (from open circuit in the dark to open circuit under illumination to short circuit under illumination) takes place in the semiconductor. The potential drop across interfacial planes is comparatively small and invariant.

All potentials given in Fig. 3 are referenced to the potential at the interface between the semiconductor and the current collector. This choice of reference potential is arbitrary, and is used here to emphasize the degree of band bending and straightening in the semiconductor. A number of researchers (see, e.g., Refs. 17 and 19) have reported that the potential of the solution is independent of current and illumination intensity when referenced to an external quantity such as the Fermi energy of an electron in vacuum. This concept does not have strict thermodynamic validity because it depends upon the calculation of individual ionic activity coefficients[38]; however, it has proved useful for the prediction of the interaction among semiconductors and a variety of redox

systems. Memming,[17,39] for example, has provided a chart of the relative energies for redox systems as compared to the valence and conduction band edge energies for several semiconductors.

Concentration distributions of holes and electrons in the semiconductor are presented in Fig. 4 for a system with no interfacial kinetic limitations. Under equilibrium conditions the concentration of holes (curve a) is essentially zero in the bulk of the semiconductor and increases near the negatively charged interface. Conduction electrons are depleted near the interface and reach a value close to unity at the current collector, where the concentrations are scaled by the dopant concentration ($N_d - N_a$), and $N_d$ and $N_a$ represent the concentrations of ionized electron donors and acceptors, respectively. The equilibrated semiconductor of Fig. 4 can therefore be described as having an inversion region extending from the semiconductor-electrolyte interface to three Debye lengths from the interface [see Eq. (20) for a mathematical definition of the Debye length], a depletion region extending from three to eight Debye

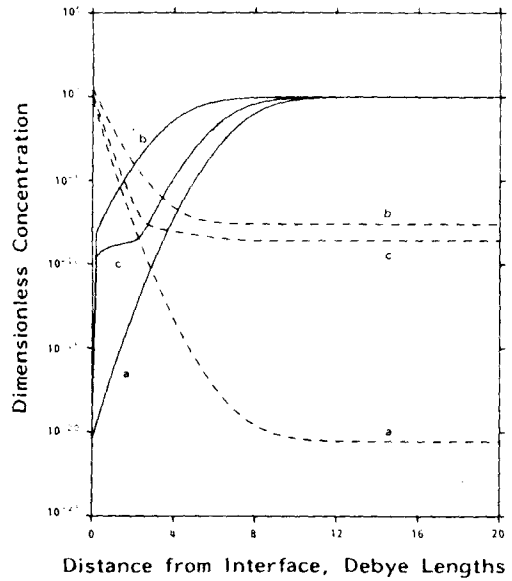


Figure 4. Concentration distribution for an *n*-GaAs rotating disk electrode with no interfacial kinetic limitations. Dashed lines, holes; solid lines, electrons; curve a, open circuit in the dark; curve b, open circuit under 882 W/m$^2$ illumination; and curve c, near short circuit ($i = -23.1$ mA/cm$^2$) under illumination. Concentrations are made dimensionless by the net dopant concentration $N_d - N_a$.



lengths, and a neutral region adjacent to the current collector. An inversion region is usually defined as the region for which the dimensionless minority carrier concentration is greater than one. The definition used here is for a region where the minority carrier concentration is greater than the majority carrier concentration.

The semiconductor described by Fig. 4 has a net positive charge which is balanced by charge associated with the diffuse region of the electrolyte and with the interface such that system electroneutrality is maintained. The potential gradient, the driving force for migration of charged species, is balanced by the concentration gradient, which drives diffusion. Thus, the net flux of each species in the semiconductor is equal to zero at equilibrium.

Illumination under open-circuit conditions produces electron-hole pairs, which are separated by the potential gradient (see Fig. 3). The concentration of holes increases near the interface, and the concentration of electrons increases near the current collector (curve b in Fig. 4). Under steady-state conditions, the rate of generation of electron-hole pairs is balanced by the rate of homogeneous and interfacial recombination. As the system without kinetic limitations approaches short circuit (curve c in Fig. 4), the concentrations of holes and electrons approach the equilibrium distributions.

The potential and concentration distributions described for the system with no kinetic limitations to interfacial reactions are constrained by the rates of generation and mass transfer in the semiconductor. More generally, kinetic limitations to interfacial reactions are compensated by the increased interfacial potential and concentration driving forces required to allow passage of electrical current. In contrast to the results shown as curve c in Fig. 4, the surface concentration of holes under kinetic limitations to interfacial reactions can increase with increasing current density.[37] The presence of these limitations may be inferred from experimental data by inflection points in the current-potential curve.

## II. MATHEMATICAL DESCRIPTION

Macroscopic transport equations are commonly used to describe the semiconductor and the electrolyte in the liquid-junction cell. A microscopic model of the semiconductor-electrolyte interface couples the equations governing the macroscopic systems.

### 1. Semiconductor

The electrochemical potential of a given species can arbitrarily be separated into terms representing a reference state, a chemical contribution, and an electrical contribution:

$$\mu_i = \mu_i^{\ominus} + RT \ln(c_i f_i) + z_i F \Phi \tag{1}$$

where $\Phi$ is a potential which characterizes the electrical state of the phase and can be arbitrarily defined. The potential used here is the electrostatic potential which is obtained through integration of Poisson's equation.[40] Equation (1) defines the activity coefficient, $f_i$.

The flux density of an individual species within the semiconductor is driven by a gradient of electrochemical potential:

$$\mathbf{N}_i = -c_i u_i \nabla \mu_i \tag{2}$$

This can be written for electrons and holes in terms of concentration and potential gradients (see, e.g., Ref. 10 or 33). The flux density of holes $\mathbf{N}_h$ is therefore given by

$$\mathbf{N}_h = \frac{u_h RT}{f_h} \nabla(p f_h) - u_h p F \nabla \Phi \tag{3}$$

and a similar result is obtained for the flux density of electrons. The concentrations of electrons and holes are represented by $n$ and $p$, respectively, and the mobilities $u_i$ are related to the diffusivities $D_i$ by the Nernst-Einstein equation, i.e.,

$$D_i = RT u_i \tag{4}$$

This equation is appropriate for both dilute and concentrated solutions.[31] Nonidealities associated with more concentrated solutions are incorporated within the activity coefficient.

Equation (3) can be simplified through the assumption of constant activity coefficients. Under the assumption of constant activity coefficients, Eq. (3) is in harmony with a Boltzmann distribution of electrons and holes. Such an approach is valid for $p/N_v$ and $n/N_c$ less than 0.1. At higher concentrations, Fermi-Dirac statistics must be used to account for the distribution of electrons and holes as functions of energy. These effects can be treated by introduction of concentration-dependent activity coefficients for



electrons and holes such as those originally presented by Rosenberg,[41-46] i.e.,

$$f_e = \frac{\exp(\eta_e)}{F_{1/2}(\eta_e)} \tag{5a}$$

and

$$f_h = \frac{\exp(\eta_h)}{F_{1/2}(\eta_h)} \tag{5b}$$

respectively, where

$$\eta_e = \frac{E_f - E_c}{kT} \tag{5c}$$

$$\eta_h = \frac{E_v - E_f}{kT} \tag{5d}$$

$E_f$ is the Fermi energy, $E_c$ and $E_v$ are the energies of the conduction and valence band edges, respectively, and $F_{1/2}(\eta)$ is the Fermi integral of order one-half for the argument $\eta$. The activity coefficients approach values of unity at dilute carrier concentration because the value of $F_{1/2}(\eta)$ approaches $\exp(\eta)$ at dilute carrier concentrations. The concentration dependency of Eqs. (5a)-(5d) can be obtained explicitly through analytic expressions relating $\exp(\eta)$ to $F_{1/2}(\eta)$.[47-50]

Equation (5) is restricted by the assumption that the energies of the band edges are independent of carrier concentration. The expressions

$$f_e = \frac{\exp(\eta_e)}{F_{1/2}(\eta_e)} \exp(-\Delta E_c'/kT) \tag{6a}$$

and

$$f_h = \frac{\exp(\eta_h)}{F_{1/2}(\eta_h)} \exp(-\Delta E_v'/kT) \tag{6b}$$

account for the interactions among electrons and holes which cause shifts in the conduction and valence band-edge energies, $\Delta E_c'$ and $\Delta E_v'$, respectively. An additional shift in band energies is associated with large concentrations of dopant species. These effects are included within material balances which couple transport and

kinetic expressions. This separation of the influence of dopant and carrier concentrations is necessary in regions where the assumption of electroneutrality is not valid. Several reviews of the influence of carrier and dopant concentrations are available (see, e.g., Refs. 51-57).

The thermodynamic consistency of the expressions used for electron and hole activity coefficients can be evaluated by application of the second cross derivative of the Gibbs function,[58] i.e.,

$$\left(\frac{\partial \mu_e}{\partial p}\right)_{T,P,n} = \left(\frac{\partial \mu_h}{\partial n}\right)_{T,P,p} \tag{7}$$

Equation (7) is properly expressed in terms of mole numbers. Under the assumption that the concentrations are sufficiently dilute to allow lattice expansion to be ignored, the thermodynamic relationship can be expressed in terms of concentrations. Application to Eq. (6) yields[59]

$$\left(\frac{\partial \Delta E_c'}{\partial p}\right)_{T,P,n} = \left(\frac{\partial \Delta E_v'}{\partial n}\right)_{T,P,p} \tag{8}$$

Equation (8) constrains the choice of expressions used to account for the influence of carrier interactions on shifts of the conduction and valence band-edge energies.

Experimental results have been used to obtain averaged activity coefficients.[60] Another approach toward characterization of degenerate semiconductors has been to include the nonidealities associated with degeneracy within a modified Nernst-Einstein relationship.[61-64] The modified Nernst-Einstein relationship is given by[65]

$$D_i = RTu_i \frac{F_{1/2}(\eta_i)}{\dfrac{\partial}{\partial \eta_i} F_{1/2}(\eta_i)} \tag{9}$$

This approach is related to the activity coefficient used in the above development by[43]

$$\frac{F_{1/2}(\eta_i)}{\dfrac{\partial}{\partial \eta_i} F_{1/2}(\eta_i)} = \left(1 + \frac{\partial \ln f_i}{\partial \ln c_i} - \frac{\partial \Delta E_i'}{\partial \ln c_i}\right) \tag{10}$$

The validity of the Nernst-Einstein relation rests on the fact that the driving force for both migration and diffusion is the gradient



of the electrochemical potential, and the decomposition of this into chemical and electrical contributions is arbitrary and without basic physical significance.[38] Correction of the Nernst-Einstein relationship to account for nonideal behavior represents a decomposition of the electrochemical potential gradient such that the diffusional flux density is proportional to the gradient of concentration, not activity as given in Eq. (3). The approach represented by Eqs. (1)-(8) allows separation of the influence of nonideal behavior from transport properties. The principal advantage of this approach is that the activity coefficients presented in Eqs. (5) and (6) can also be employed within the framework of the transport theory for concentrated solutions.[33,66]

Homogeneous reaction takes place in the semiconductor; thus a material balance for a given species, say holes, yields

$$\nabla \cdot \mathbf{N}_h = R_h \tag{11}$$

where $R_h$ is the net rate of production of holes under steady-state conditions. The rate of production of holes is, by stoichiometry, equal to the rate of production of electrons and is governed by three concurrent processes: generation by absorption of light, generation by absorption of heat, and recombination of electrons and holes (i.e., transfer of an electron from the conduction band to the valence band):

$$R_h = G_L + G_{\text{th}} - R_{rec} \tag{12}$$

Mathematical models of the homogeneous recombination process have been developed which incorporate single-step electron transfer from one energy level to another. They differ in the assumption of the presence or absence of impurities which allow electrons to have energies between the conduction and valence-band energies.[67-69]

Band-to-band kinetic models (presented in Fig. 5) allow electrons to have only valence or conduction-band energies. Absorption of the appropriate amount of thermal or electromagnetic energy creates an electron-hole pair; recombination of an electron and a hole releases energy in the form of heat or light. The band-to-band model yields

$$R_h = \eta m q_0 e^{-my} - k_{\text{rec}}(np - n_i^2) \tag{13}$$

where $\eta$ is the fraction of incident photons with energy greater

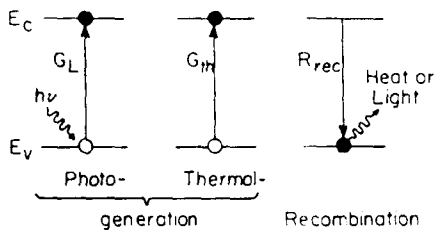


Individual Reaction Rates

$$G_{th} = k_{th}(N_c - n)(N_v - p)$$

$$R_{rec} = k_{rec}\, np$$

Figure 5. Schematic representation of band-to-band recombination kinetics in the semiconductor.

than the band gap energy, $m$ is the absorption coefficient, $q_0$ is the incident solar flux, and $n_i$ is the intrinsic concentration,

$$n_i = \left[\frac{k_{th}(N_c - n)(N_v - p)}{k_{rec}}\right]^{1/2} \tag{14}$$

The intrinsic concentration is written in terms of $N_c$ and $N_v$, the number of available conduction and valence-band sites, respectively, and $k_{th}$ and $k_{rec}$, thermal generation and recombination rate constants. Under equilibrium conditions, the rate of thermal generation is equal to the rate of recombination, and $np = n_i^2$.

Most semiconducting materials contain within their lattice structure impurities or imperfections which may be described as fixed sites with valence-band electron energies within the semiconductor band gap. The trap-kinetics model allows recombination to occur through these sites (see Fig. 6). Absorbed radiation drives an electron from the valence band to the conduction band, and all recombination and thermal generation reactions are assumed to occur though trap sites. This model results in

$$R_h = \eta m q_0\, e^{-my} - \frac{N_t k_2(np - n_i^2)}{\dfrac{k_1(N_v - p) + k_3(N_c - n)}{k_4} + \dfrac{k_2}{k_4}p + n} \tag{15}$$

where $k_1$, $k_2$, $k_3$, and $k_4$ are the rate constants for reactions 1-4,



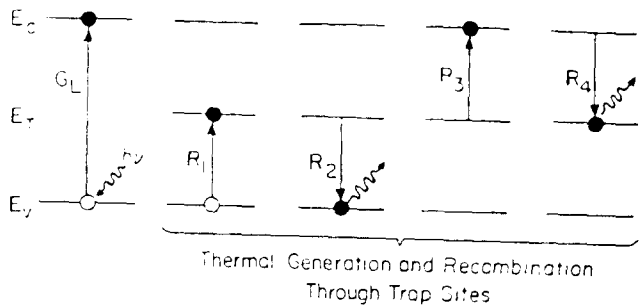


Individual Reaction Rates

$$R_1 = k_1(N_v - p)(N_T - n_T)$$

$$R_2 = k_2 n_T p$$

$$R_3 = k_3 n_T (N_c - n)$$

$$R_4 = k_4 n (N_T - n_T)$$

Figure 6. Schematic representation of single-trap recombination kinetics in the semiconductor (Ref. 36). Reprinted by permission of the publisher, the Electrochemical Society, Inc.

respectively, shown in Fig. 6. The intrinsic concentration is given by

$$n_i = \left[\frac{k_1 k_3(N_c - n)(N_v - p)}{k_2 k_4}\right]^{1/2} \tag{16}$$

The expressions for the intrinsic concentration [Eqs. (13) and (16)] are consistent with the expression derived through statistical-mechanical models, e.g.,

$$np = n_i^2 = (N_c - n)(N_v - p)\, e^{-E_g/kT}$$

The intrinsic concentration can be considered to be a constant for a given semiconductor only if the ratios $n/N_c$ and $p/N_v$ are negligibly small compared to unity. The intrinsic concentration is related to the nondegenerate limit $n_{lim}$ and the activity coefficients of Eqs. (5) and (6) by

$$n_i = n_{lim}\left(\frac{1}{f_e f_h}\right)^{1/2} \exp(\Delta E_g/kT) \tag{17}$$

where $\Delta E_g$ represents the narrowing of the band gap associated

with large dopant concentrations. The assumption of a constant intrinsic concentration is consistent with the assumption of unity activity coefficients for electrons and holes. The value of the intrinsic concentration derived from statistical-mechanical arguments serves as a relationship among the kinetic parameters in Eqs. (14) and (16).

The divergence of the current is zero at steady state; therefore the fluxes of holes and electrons are related by

$$\nabla \cdot \mathbf{N}_e - \nabla \cdot \mathbf{N}_h = 0 \tag{18}$$

A material balance on electrons, analogous to Eq. (11), could be used to replace Eq. (18). Numerical computational accuracy is enhanced by coupling conservation of the minority carrier with Eq. (18).

Poisson's equation,

$$\nabla^2 \Phi = -\frac{F}{\varepsilon_{sc}}[p - n + (N_d - N_a)] \tag{19}$$

relates the potential to the charge distribution. The Debye length,

$$\lambda_{sc} = [\varepsilon_{sc} RT / F^2 (N_d - N_a)]^{1/2} \tag{20}$$

characterizes the distance over which the potential varies in the semiconductor. It typically has a value of 10 to 200 nm.

The degree of ionization of donors or acceptors is dependent upon the concentrations of charged species within the semiconductor and upon the temperature. Complete ionization is frequently assumed, and this assumption is reasonable at room temperatures. Gerischer[70] presents development of these equations under the condition of incomplete dopant ionization.

## 2. Electrolyte

The equations which govern the electrolyte are similar to those which govern the semiconductor with the exceptions that homogeneous reactions can frequently be neglected and that convective transport of ionic species may be important. For dilute electrolytic solutions (less than 3 $M$) the flux density of an ionic species can be expressed in terms of migrational, diffusional, and convective components, i.e.,

$$\mathbf{N}_i = -z_i u_i c_i F \nabla \Phi - D_i \nabla c_i + c_i \mathbf{v} \tag{21}$$



This relationship fails for concentrated solutions owing to the neglect of the contributions of activity coefficients [see Eq. (3)] and to the neglect of ion–ion interactions.[33] Under the assumptions of steady state and that homogeneous reactions can be neglected, Eq. (11) can be expressed as

$$\nabla \cdot \mathbf{N}_i = 0 \tag{22}$$

The expression of Poisson's equation is analogous to Eq. (19), i.e.,

$$\nabla^2 \Phi = -\frac{F}{\varepsilon_{sol}} \sum_i z_i c_i \tag{23}$$

Electroneutrality of the electrolyte is not assumed here because the charge held within the diffuse region near the interface can be significant, and this charge contributes to balancing the charge held within the space-charge region of the semiconductor. The Debye length in the solution is given by

$$\lambda_{sol} = \left( \frac{\varepsilon_{sol} RT}{F^2 \sum_i z_i c_{i,\infty}} \right)^{1/2} \tag{24}$$

and typically has a value of 0.1 to 1 nm.

The charge held within the diffuse part of the double layer approaches zero far from the interface. The distance over which this charge approaches zero is scaled by the Debye length. At distances greater than 20 Debye lengths, Eq. (23) can be replaced by the requirement of electroneutrality:

$$\sum_i z_i c_i = 0 \tag{25}$$

The characteristic scaling distance for the diffusion layer (see Ref. 33) is much larger than the Debye length; therefore efficient numerical treatment of the influence of electrolytic mass transfer on the performance of photoelectrochemical cells requires a change of scale at the inner limit of the diffusion layer (or the outer limit of the diffuse part of the double layer).

The relationship presented above are sufficient to describe the electrolytic solution. An additional relationship yields the current density as a function of the ionic fluxes,

$$i = F \sum_i z_i \mathbf{N}_i \tag{26}$$

Within the semiconductor, this can be regarded to be an integrated form of Eq. (18).

### 3. Semiconductor–Electrolyte Interface

The interfacial reactions described in Section I.1 are driven by departure from equilibrium. For a general interfacial reaction given by[33]

$$\sum_i s_i M_i^{z_i} \rightarrow 0 \tag{27}$$

the condition of equilibrium is given by

$$\sum_i s_i \mu_i = 0 \tag{28}$$

Here, $s_i$ is the stoichiometric coefficient of species $i$, $M_i$ is a symbol for the chemical formula of species $i$, and $\mu_i$ is the electrochemical potential of species $i$. Electrons at a given energy level (or holes) are included explicitly as a reactant.

The rate of reaction $l$ at the interface is given by

$$r_l = k_{f,l} \exp\left[\frac{(1-\beta_l) n F \Delta\Phi_l}{RT}\right] \prod_i c_i^{p_{i,l}} - k_{b,l} \exp\left(\frac{-\beta_l n F \Delta\Phi_l}{RT}\right) \prod_i c_i^{q_{i,l}} \tag{29}$$

where $\beta_l$ is a symmetry factor (usually assumed to be equal to 1/2), $k_{f,l}$ and $k_{b,l}$ are forward and backward reaction rate constants, respectively, $n$ is the number of electrons transferred, and $\Delta\Phi_l$ is the potential driving force for the given reaction, $l$. The potential driving force enters into reactions involving charge transfer from locations of one potential to locations of another.

The reaction orders for a given species $i$ in the forward and reverse directions are $p_{i,l}$ and $q_{i,l}$, respectively. They are determined from the stoichiometric coefficients, $s_{i,l}$:

For $s_{i,l} = 0$: $p_{i,l} = 0$ and $q_{i,l} = 0$

For $s_{i,l} > 0$: $p_{i,l} = s_{i,l}$ and $q_{i,l} = 0$

For $s_{i,l} < 0$: $p_{i,l} = 0$ and $q_{i,l} = -s_{i,l}$



The reaction rates are written in terms of the equilibrium constants as

$$r_l = k_{b,l}\left\{ K_l \exp\left[\frac{(1-\beta_l) F \Delta\Phi_l}{RT}\right] \prod_i c_i^{p_{i,l}} - \exp\left(\frac{-\beta_l F \Delta\Phi_l}{RT}\right) \prod_i c_i^{q_{i,l}} \right\} \tag{30}$$

The equilibrium constant used here is the ratio of the forward and backward rate constants:

$$K_l = \frac{k_{f,l}}{k_{b,l}} \tag{31}$$

The equilibrium constants can be related to equilibrium interfacial concentrations and potentials, i.e.,

$$K_l = \exp\left(-\frac{F}{RT}\Delta\Phi_l\right) \prod_i c_i^{-s_{i,l}} \tag{32}$$

Through Eq. (30), the equilibrium constants can be related to electron-site and Fermi energies. Within parametric studies, it is convenient to allow one independent rate constant to be characteristic of each group of interfacial reactions. For example, adsorption reactions (IHP–OHP) might have individual rate constants for each reaction $l$ related to the characteristic rate constant by

$$k_{b,l} = k_j^0 K_l^{-1/2} \tag{33a}$$

and

$$k_{f,l} = k_j^0 K_l^{1/2} \tag{33b}$$

where $k_j^0$ is the preexponential part of the rate constant, with a characteristic value for a given reaction type $j$, and $\beta$ was given a value of one half. The value for the equilibrium constant $K_l$ incorporates the energy levels of interfacial sites and associated energies of adsorption. These equations are consistent with Eqs. (30) and (31).

The general approach described above can be applied to an arbitrarily complex interfacial reaction scheme. Concentrations of reacting species are related to surface reactions by material balances which, under steady-state conditions, are expressed by continuity

of flux at the OSS and the OHP; i.e.,

$$\mathbf{N}_e\Big|_{\text{OSS}} = \sum_l - s_{e,l} r_{l,\text{OSS}} \tag{34a}$$

$$\mathbf{N}_h\Big|_{\text{OSS}} = \sum_l - s_{h,l} r_{l,\text{OSS}} \tag{34b}$$

and

$$\mathbf{N}_i\Big|_{\text{OHP}} = \sum_l - s_{i,l} r_{l,\text{OHP}} \tag{34c}$$

Material balances are also written for each adsorbed species $i$ at the ISS and the IHP, i.e.,

$$\sum_l s_{i,l} r_{l,\text{ISS}} = 0 \tag{35a}$$

and

$$\sum_l s_{i,l} r_{l,\text{IHP}} = 0 \tag{35b}$$

These equations apply only if surface states are involved within the microscopic model of the interface.

Gauss's law can be applied to the region between the OSS and ISS:

$$\Phi_{\text{OSS}} - \Phi_{\text{ISS}} = \frac{\delta_1}{\varepsilon_{\text{sc}}}\left[\frac{\varepsilon_1}{\delta_2}(\Phi_{\text{ISS}} - \Phi_{\text{IHP}}) + F\sum_{\text{ISS}} z_i\Gamma_i\right] \tag{36a}$$

and between the ISS and the IHP:

$$\Phi_{\text{ISS}} - \Phi_{\text{IHP}} = \frac{\delta_2}{\varepsilon_2}\left[\frac{\varepsilon_{\text{sol}}}{\delta_3}(\Phi_{\text{IHP}} - \Phi_{\text{OHP}}) + F\sum_{\text{IHP}} z_i\Gamma_i\right] \tag{36b}$$

where $\Gamma_i$ are the surface concentrations of charged species located at the respective interfacial planes.

The approach described above allows description of interfacial reactions in terms of individual single-step processes. Frequently, reactions are described by a single rate expression. The rate of a charge-transfer reaction, for example, can be expressed through



the Marcus-Gerischer theory by

$$\begin{aligned} r = {} & k_{\text{red}} c_{\text{red}} \int_{-\infty}^{+\infty} \kappa(E)\rho(E)[1 - f(E)]D_{\text{red}}(E)\,dE \\ & - k_{\text{ox}} c_{\text{ox}} \int_{-\infty}^{+\infty} \kappa(E)\rho(E)f(E)D_{\text{ox}}(E)\,dE \end{aligned} \tag{37}$$

where $k_{\text{ox}}$ and $k_{\text{red}}$ are rate constants, $\kappa(E)$ is an energy-dependent transmission or rate constant, $\rho(E)[1 - f(E)]$ is the distribution of unoccupied electron states in the electrode, $\rho(E)f(E)$ is the distribution of occupied states in the electrode, and $D_{\text{ox}}$ and $D_{\text{red}}$ are the distributions of occupied and unoccupied states, respectively, for electrons associated with the ionic species.[10,17,70] This may be regarded to be a form of Eq. (29) integrated over all electron energy levels. Within this approach, the occupancy of electron states $f(E)$ is given by the Fermi-Dirac distribution, and the energy states of electrons associated with ionic species are distributed according to

$$D_{\text{red}}(E) = \exp\left[-\frac{(E - E_{F,\text{el}} - \lambda)^2}{4kT\lambda}\right] \tag{38a}$$

and

$$D_{\text{ox}}(E) = \exp\left[-\frac{(E - E_{F,\text{el}} + \lambda)^2}{4kT\lambda}\right] \tag{38b}$$

where $\lambda$ is called the rearrangement or reorientation energy. This term is used to relate the energy of electrons in the semiconductor to the energy of electrons associated with the ionic species. At equilibrium, the Fermi energy, or electrochemical potential, of electrons in the semiconductor is equal to the Fermi energy of electrons associated with the ionic species. This requirement specifies the concentrations of oxidized and reduced species at the semiconductor surface.

A kinetic argument can be used instead to establish the equilibrium distribution of ions at the semiconductor surface. The rate of adsorption of a species $i$ is given according to Eq. (29) as

$$\begin{aligned} r_l = {} & k_{f,l} \exp\left[\frac{-z_i(1 - \beta_l)F\Delta\Phi_l}{RT}\right]\Gamma_i \\ & - k_{b,l} \exp\left(\frac{z_i\beta_l F\Delta\Phi_l}{RT}\right) c_i\left(\Gamma_{\text{IHP}} - \sum_k \Gamma_k\right) \end{aligned} \tag{39}$$

Under equilibrium conditions the reaction rate is zero, and the fractional occupation of the inner Helmholtz plane is given by

$$\frac{\Gamma_i}{\Gamma_{IHP}} = \frac{c_i e^{-\Delta E_i/RT}}{1 + \sum_k c_k e^{-\Delta E_k/RT}} \tag{40}$$

where

$$\Delta E_i = -z_i F \Delta\Phi_l + RT \ln\left(\frac{k_{f,l}}{k_{b,l}}\right) \tag{41}$$

The fractional occupation by a single species $i$ corresponds to that given by the Langmuir adsorption isotherm (see, e.g., Delahay[71]) for which $\Delta E_i$ is the "standard" free energy of adsorption. The "standard" free energy of adsorption is therefore a function of $\Delta\Phi_l$, the equilibrium potential difference between the inner and outer Helmholtz planes.

The equilibrium constants given in Eq. (32) couple the equilibrium concentrations of electrons, obtained as functions of Fermi energy, and the equilibrium concentrations of adsorbed ions, obtained as functions of concentration and free energies of adsorption.

## 4. Boundary Conditions

The boundary conditions are specified by the microscopic model of the various interfaces included within the photoelectrochemical cell. A metal-semiconductor interface, for example, can be described in a manner similar to that presented in the preceding section. Consider a semiconducting electrode bounded at one end by the electrolyte and at the other end by a metallic current collector. The boundary conditions at the semiconductor-electrolyte interface are incorporated into the model of the interface. Appropriate boundary conditions at the semiconductor-current collector interface are that the potential is zero, the potential derivative is equal to a constant, determined by the charge assumed to be located at the semiconductor-current collector interface, and all the current is carried by electrons (the flux of holes is zero). These conditions are consistent with a *selective ohmic contact*.[34] The boundary conditions in the electrolytic solution may be set a fixed distance from



the interface. If this location is considered to be the other limit of the diffusion layer, the appropriate boundary conditions are that the potential gradient is continuous and that all concentrations have their bulk value. The electrostatic potential can be set to an arbitrary value at this point.

It is common to treat the semiconductor-electrolyte interface in terms of charge and current density boundary conditions. The total charge held within the electrolytic solution and the interfacial states, which balances the charge held in the semiconductor, is assumed to be constant. This provides a derivative boundary condition for the potential at the interface. The fluxes of electrons and holes are constrained by kinetic expressions at the interface. The assumption that the charge is constant in the space charge region is valid in the absence of kinetic and mass-transfer limitations to the electrochemical reactions. Treatment of the influence of kinetic or mass transfer limitations requires solution of the equations governing the coupled phenomena associated with the semiconductor, the electrolyte, and the semiconductor-electrolyte interface.

## 5. Counterelectrode

In the region sufficiently far from the interface that electroneutrality holds and under the assumptions that the concentration is uniform and that the solution adjacent to the electrodes may be treated as equipotential surfaces, the potential distribution can be obtained through solution of Laplace's equation, $\nabla^2\Phi = 0$, and is a function of current density. The potential drop in the region between the counterelectrode and the outer limit of the diffusion layer is given by

$$V_{IR} = \frac{Li}{\kappa} \tag{42}$$

where $\kappa$ is the solution conductivity and $L$ is the distance between the counterelectrode and the outer edge of the diffusion layer. The counterelectrode was assumed here to be in a configuration parallel to the semiconductor. Relaxation of this assumption will be discussed in Section III.3. The conductivity of dilute solutions can be related to ionic mobilities and concentrations by

$$\kappa = F^2 \sum_i z_i^2 u_i c_i \tag{43}$$

or is obtained from experimental measurements for a given electrolyte.

The potential drop across the counterelectrode-electrolyte interface is given by

$$V_{CE} = V^0_{CE} + \eta_{CE} \tag{44}$$

where $V^0_{CE}$ is the equilibrium potential drop across the interface and $\eta_{CE}$ is the total counterelectrode reaction overpotential. The total overpotential is related to the current density through the Butler-Volmer reaction model[33,71]

$$i = i_0\left\{\left(1 - \frac{i}{i_{c,\lim}}\right)\exp\left[\frac{(1-\beta)nF}{RT}\eta_{CE}\right] - \left(1 + \frac{i}{i_{a,\lim}}\right)\exp\left(-\frac{\beta nF}{RT}\eta_{CE}\right)\right\} \tag{45}$$

where $i_0$ is the exchange current density associated with the bulk concentrations of reactants, $i_{k,\lim}$ is the diffusion-limited current density associated with species $k$, and $n$ is the number of electrons transferred in the counterelectrode reaction.

## III. PHOTOELECTROCHEMICAL CELL DESIGN

The liquid-junction photovoltaic cell has the advantages that the junction between electrolytic solution and semiconductor is formed easily and that polycrystalline semiconductors can be used. The principal disadvantage is that the semiconductor electrode tends to corrode under illumination. The electrochemical nature of the cell allows both production of electricity and generation of chemical products which can be separated, stored, and recombined to recover the stored energy. Liquid-junction cells also have the advantages that are attributed to other photovoltaic devices. Photovoltaic power plants can provide local generation of power on a small scale. The efficiency and cost of solar cells is independent of scale, and overall efficiency is improved by locating the power plant next to the load.[72]

The design of a liquid-junction photovoltaic cell requires selection of an appropriate semiconductor-electrolyte combination and



design of an efficient cell configuration. The selection of a semiconductor is based upon the band gap, which provides an upper limit to the conversion efficiency of the device, and the choice of electrolyte is governed by the need to limit corrosion and by the requirement that interfacial reaction rates be fast.

### 1. Choice of Materials

The performance of photoelectrochemical cells constructed with thin-film or polycrystalline semiconductors is strongly dependent upon the method of film formation and upon the surface preparation. Conversion efficiencies (incident solar illumination to electrical power) of 3%–6.5% have been reported for cells using thin-film $n$-CdSe electrodes (see Refs. 73–81), and a conversion efficiency of 5.1% has been achieved with a pressure-sintered polycrystalline CdSe photoelectrode.[82] A comparable efficiency of 8.1% has been reported for a single-crystal CdSe electrode.[83] Conversion efficiencies of 0.038%–0.3% have been reported for polycrystalline CdS films[84–86] as compared to 1.3% for single-crystal CdS.[87] Conversion efficiencies of up to 7.3% have been reported for polycrystalline $n$-GaAs films[88–90]; 12% has been reported for the single crystal $n$-GaAs.[91,92] For descriptions of other semiconductor electrolyte combinations see Refs. 93–104. The lower efficiency of the polycrystalline thin-film semiconductors, as compared to the single-crystal counterparts, is expected to be compensated by their lower cost. Reviews of the materials aspects of photoelectrochemical cells are given in Refs. 105–107.

#### *(i) Band Gap*

An upper limit to the efficiency of photovoltaic devices can be established, based upon the band gap and the solar spectrum, without consideration of cell configuration. This ultimate efficiency is given by[11]

$$\eta_{ult} = \frac{E_g \int_{E_g}^{\infty} N(E)\,dE}{\int_0^{\infty} EN(E)\,dE} \tag{46}$$

where $E_g$ is the semiconductor band-gap energy, $E$ is the photon energy, and $N(E)$ is the number density of incident photons with

energy $E$. The fraction of the power in the solar spectrum that can be converted to electrical power is a function of the band gap of the semiconductor. Photons with energy less than the band gap cannot produce electron–hole pairs. Photons with energy greater than the band gap yield only the band gap energy.[108-110]

The ultimate efficiency of Eq. (46) represents an upper limit to conversion of solar energy[10,111,112]; factors such as reflection and absorption losses of sunlight, kinetic and mass transfer limitations, and recombination will reduce the efficiency. These effects are included in Section III.3. A band gap between 1.0 and 1.5 eV is generally considered to be appropriate for efficient conversion of solar energy.

### *(ii) Corrosion*

The application of liquid-junction technology to photovoltaic power conversion is limited by problems associated with the semiconductor–electrolyte interface. Primary among these problems is corrosion. Efficient conversion of solar energy requires a band gap between 1.0 and 1.5 eV, and most semiconductors near this band gap corrode readily under illumination. Semiconductors with large band gaps (4–5 eV) tend to be more stable but cannot convert most of the solar spectrum.

Among the approaches taken to solve this problem, the most successful concern the matching of an electolyte to the semiconductor. The rate of corrosion is reduced if the semiconductor is in equilibrium with the corrosion products. The rate of corrosion can also be reduced by using a redox couple which oxidizes easily. The oxidation of the redox couple $Se^{2}_{x+1}/Se^{2}_{x}$ for example, has been shown to compete successfully with photocorrosion reactions for holes in $n$-type GaAs electrodes.[28,113-116]

$p$-type semiconductors used as cathodes are more stable than the more common and generally more efficient $n$-type semiconducting anodes. The inefficiency of $p$-type photocathodes has been attributed to the presence of surface states near the valence band energy. A stable $p$-type photocathode has been developed, however, with a solar-energy-conversion efficiency of 11.5%.[117] Protective films have been proposed to be a solution to electrode corrosion. The electrode, in this case, would be a small band-gap semiconductor covered by a film composed of either a more stable large band-gap semiconductor,[118] a conductive polymer, or a metal. A large Schottky barrier is frequently present at such semiconductor–metal and semiconductor–semiconductor interfaces which blocks the transfer of holes from the semiconductor to the electrolyte. In cases where the photocurrent is not blocked, corrosion can take place between the semiconductor and the protective film.[40,119] Menezes *et al.*[120] discuss the difficulties in avoiding absorptive losses in the metal film while maintaining sufficient integrity to serve the semiconductor corrosion protection function. Frese *et al.*[121] have, however, reported a measurable improvement in the stability of GaAs with less than a monolayer gold metal coverage. Thin conductive poly-pyrrole films appear to be successful in inhibiting corrosion in some electrolytes.[122-128] In addition, insulating polymer films deposited on grain boundaries can improve the performance of polycrystalline semiconductors by reducing surface recombination rates.[129,130] (For more complete reviews of the corrosion of semiconducting electrodes, see Refs. 18, 19, 28, 131, and 132.)



## 2. Solution of the Governing Equations

Quantitative optimization or prediction of the performance of photoelectrochemical cell configurations requires solution of the macroscopic transport equations for the bulk phases coupled with the equations associated with the microscopic models of the interfacial regions. Coupled phenomena govern the system, and the equations describing their interaction cannot, in general, be solved analytically. Two approaches have been taken in developing a mathematical model of the liquid-junction photovoltaic cell: approximate analytic solution of the governing equations and numerical solution.

### *(i) Analytic Approach*

The semiconductor electrode is typically divided into three regions. Surface-charge and electron and hole-flux boundary conditions model the semiconductor–electrolyte interface. The region adjacent to the interface is assumed to be a depletion layer, in which electron and hole concentrations are negligible. The potential

variation is therefore independent of hole and electron concentration in this region. Far from the interface a neutral region is defined in which the potential is constant; here electron and hole fluxes are driven only by diffusion. Current-potential relationships are derived in the analytic approach by invoking assumptions appropriate to each region.

Integration of Poisson's equation in the depletion layer, for example, results in a depletion layer thickness $W$ in terms of the voltage drop $V$ across the layer:

$$W = \left[\frac{2\varepsilon V}{F(N_d - N_a)}\right]^{1/2} \tag{47a}$$

This can also be written in terms of the charge $q$ held within the space-charge region

$$W = \frac{q}{F(N_d - N_a)} \tag{47b}$$

or

$$V = \frac{q^2}{2\varepsilon F(N_d - N_a)} \tag{47c}$$

The depletion layer thickness is, as shown in Fig. 3, a function of illumination intensity. The assumption that the semiconductor can be separated into depletion and neutral regions restricts the voltage drop $V$ to values high enough to deplete the majority carriers (electrons in an $n$-type semiconductor) in a region adjacent to the interface but small enough to avoid formation of an inversion layer (in which the concentration of minority carriers is significant). This assumption is not appropriate under many operating conditions for which the liquid-junction cell may be practical. (Figure 4, for example, shows an inversion layer adjacent to the solution interface.)

Analytic models of photoelectrochemical devices closely resemble models of solid-state solar cells (see, e.g., Refs. 133–145). Several analytic current-voltage relationships have been derived which use the general approach described above and differ in their treatment of surface reactions and recombination within the depletion and neutral layers. The model of Gärtner,[146] developed for a $p$–$n$ junction device, is commonly used in the analysis of photoelectrochemical devices.[147–149] Recombination and thermal generation



of carriers was neglected in the interfacial and space-charge regions, but was included in the neutral region. The influence of photogenerated carriers on the potential distribution is not treated explicitly; therefore this model applies only in the region where the potential distribution approaches the equilibrium condition. Gärtner's model can be used near the short circuit condition but not at open circuit under illumination (see Fig. 3). Wilson[150,151] included recombination at the semiconductor-electrolyte interface and in the neutral region, but neglected recombination in the space-charge region. The perturbation of the potential distribution by photogenerated carriers was also neglected. Albery *et al.*[152–154] extended the model of Gärtner by including recombination of holes and electrons in the depletion layer. Reichman[155,156] presented a model which included recombination in the depletion region and kinetic limitation at the interface. Reiss[157] presented models for various cases, including within the model the potential drop across the electrolyte double layer, surface recombination, and surface kinetic limitations. The semiconductor was divided into depletion and neutral regions, and the effect of illumination on cell potential was included as an additive photovoltage. Ahlgren[158] incorporated a Butler-Volmer reaction rate expression into the boundary conditions at the semiconductor-electrolyte interface. McCann and Haneman[159] included enhanced recombination associated with grain boundaries within the bulk of the semiconductor. The photovoltage was included in the calculation of the depletion region width. McCann *et al.*[160] used an analytic model to calculate the current-voltage characteristics of front and back-wall-illuminated liquid-junction cells.

Surface states and crystal imperfections have been found to play an important role in charge-transfer and redox reactions at the semiconductor-electrolyte interface (see Refs. 161–173). Mathematical and conceptual relationships have been developed which describe electrochemical reactions at the semiconductor-electrolyte interface in terms of surface states and potentials (see, e.g., Refs. 17, 71, and 174–182). Electrochemical reaction via surface states has been included within an analytic model,[183] but this model is still limited by the restrictions described above.

Equivalent circuit models of the liquid-junction cell have also been presented.[184–186] These models are useful in the analysis of impedance response measurements.

### *(ii) Numerical Approach*

Use of a digital computer in the numerical solution of the equations governing the liquid-junction cell eliminates the need for restrictive assumptions. This approach has been used in the modeling of solid-state devices.[187-196] Laser and Bard[197-200] developed a computer program which was used to calculate open-circuit photopotentials, the transient behavior of the system following charged injection, and the time dependence of photocurrents in liquid-junction cells. Time-dependent material balances of holes and electrons and Poisson's equation described the semiconductor. The interface was included in terms of charge and flux boundary conditions. The model was limited by lack of convergence for electrode thicknesses greater than that of the space-charge region and did not treat explicitly the electrolyte and counterelectrode. Orazem and Newman[35-37] presented a numerical solution of the governing equations that included analysis of neutral, space-charge, and inversion regions in the semiconductor coupled with explicit treatment of the electrolyte and the counterelectrode. Interfacial reactions were treated explicitly; however, limitations to electrolytic mass transfer were not included in the analysis. Potential-dependent concentration variables were defined to reduce the numerical difficulties associated with concentrations that can vary up to 20 orders of magnitude in a short distance.[35,201] Errors associated with matching of solutions for various regions of the semiconductor were thereby avoided. Numerical methods for solving coupled ordinary differential equations are discussed by Newman and associates,[202,203] and a general method for treating boundary conditions is presented by White.[204]

A number of computer programs related to the liquid-junction photovoltaic cell have been developed. Leary *et al.*[205] for example, calculated carrier concentrations in polycrystalline films using a numerical solution of Poisson's equation coupled with overall charge neutrality within spherical grains. Their model was used for analysis of semiconductor gas sensors. Davis and colleagues[206-208] presented a computer program which uses simultaneous calculation of surface and solution equilibrium states to obtain the equilibrium condition of electrical double layers.



## 3. The Influence of Cell Design

The optimal design of liquid-junction photovoltaic cells shares constraints with solid-state photovoltaic cells.[25,209] Current collectors cast shadows and can reduce the amount of sunlight absorbed in the semiconductor. A constraint unique to the liquid-junction cell is the placement of the counterelectrode relative to the semiconductor–electrolyte interface. Shadows, which reduce efficiency and cause local currents in solid-state photovoltaic cells, may lead to localized corrosion in photoelectrochemical cells. Mass-transfer and kinetic limitations at the counterelectrode and resistance of the electrolyte can play important roles in the optimal design of the liquid-junction photovoltaic cell. These considerations are treated qualitatively by Parkinson.[210]

Ideally, modeling and optimization of photoelectrochemical cell configurations involves solution of the governing equations in three dimensions. A first approach toward the analysis of these devices involves coupling the solution of the one-dimensional equations (see the previous section) with primary resistance calculations for the specific cell configuration. The computational problem is still difficult but can be solved. This approach toward calculation of the influence of cell design is illustrated below and is based on the work of Orazem and Newman.[211] The system modeled was an *n*-type GaAs semiconducting anode in contact with an 0.8 *M* $K_2Se$, 0.1 *M* $K_2Se_2$, 1.0 *M* KOH electrolytic solution. The choice of this semiconducting electrode system was based upon the work of Heller and associates.[28] The semiconductor was assumed to be in the form of a thin film (see Mitchell for a review of thin-film photovoltaic technologies[29]). Interfacial reactions were included but were not limited by kinetics.[35-37] This approach requires calculation of the resistance to current flow associated with the two-dimensional systems. Some methods for calculation of this resistance were reviewed by Fleck *et al.*[212] Kasper,[213-217] Moulton,[218] Newman,[219] and Orazem and Newman[220] have presented primary resistance calculations for configurations of potential application to photoelectrochemical cells.

The design of a photoelectrochemical configuration is illustrated here for the slotted-semiconductor electrode presented in

Fig. 7a. A glass cover plate protects the cell. Sunlight passes through the cover plate and the electrolyte to illuminate the semiconductor surface. Electrical current passes between the semiconductor and the counterelectrode through slots cut in the semiconductor. Characteristic features of this configuration are that no shadows are cast upon the semiconductor and that reaction products could be separated if a membrane were placed between the semiconductor and the counterelectrode.

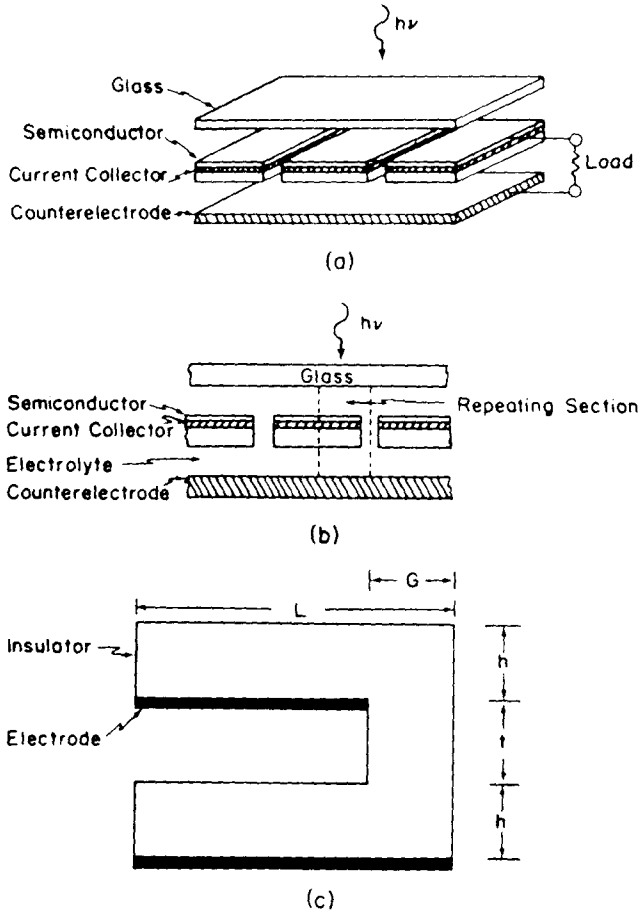


Figure 7. Slotted-electrode photoelectrochemical cell: (a) three-dimensional configuration, (b) two-dimensional representation, and (c) repeating section.



A two-dimensional representation of this cell is presented in Fig. 7b. The primary current distribution and the resistance of a cell containing a slotted electrode were calculated using numerical methods coupled with the Schwarz-Christoffel transformation.[220-222] The cell resistance is a function of three geometric ratios, chosen to be $t/G$, $h/G$, and $L/h$, where $L$ is the half-length of the protruding electrode assembly, $t$ is the thickness of the protruding electrode assembly, $G$ is the half-gap between the electrode assemblies, and $h$ is the separation between the electrode and the upper insulating wall. The separation between the counterelectrode and the lower edge of the semiconductor-electrode assembly is also given by $h$. These parameters are shown in Fig. 7c.

Four geometric parameters characterize this cell design. The distance between the counterelectrode and the semiconductor was chosen to be 0.5 cm, and the semiconductor assembly thickness was assumed to be 0.1 cm. The values chosen for this analysis were based on mechanical considerations. Smaller spacing could result in shorting of counterelectrode and semiconductor and/or trapping of gas bubbles. The influence of the counterelectrode could be reduced by increasing the flow rate or degree of mixing near the counterelectrode, thereby increasing the limiting current. Interfacial reactions were considered to be equilibrated. Kinetic limitations at the semiconductor-electrolyte interface may greatly reduce the performance of some semiconductor systems.

The primary resistance for this system is presented in Fig. 8 as a function of $L/D$ with $h/G$ as a parameter. The maximum power density is presented in Fig. 9 as a function of $L/h$ with $h/G$ as a parameter. The maximum power density for this system is obtained with a small gap. For $h/G = 0.5$ ($G = 1$ cm), the maximum power density was 47.8 W/m$^2$, and the maximum power efficiency was 5.4%. The current density under maximum power conditions was 15 mA/cm$^2$ delivered at 477.6 mV. For $h/G = 10$. ($G = 0.05$ cm), the maximum power density was 67.7 W/m$^2$, and the maximum power efficiency was 7.7%. At maximum power the current density was 15.2 mA/cm$^2$ delivered at 534.6 mV.

The hierarchy of photovoltaic cell efficiencies is presented in Table 1. Semiconductor effects, such as recombination, reduce the power efficiency of a GaAs-based device from a value of 37%, based solely upon band gap, to 15.3%. Reflection losses, with an

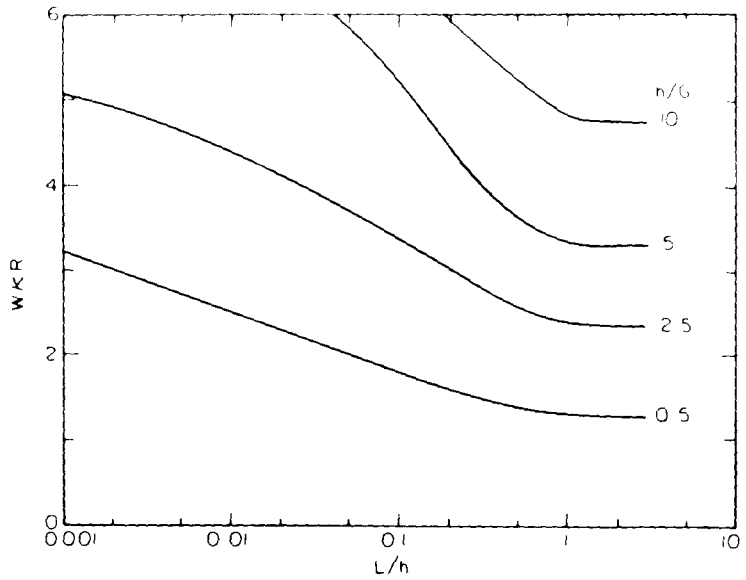


Figure 8. Primary resistance of a slotted-electrode cell as a function of $L/h$ (Ref. 211). Reprinted by permission of the publisher, the Electrochemical Society, Inc.

arbitrarily chosen 80% efficiency of illumination, reduce this value to 12.2%. This value is consistent with the value measured in a bench-top experimental system for which the influence of counterelectrode limitations and electrolyte resistance can be minimized. This value can also be compared to the 12% efficiency obtained in the experimental work of Heller and Miller.[28,91,92] Accounting for the effect of cell design reduces the efficiency from 15.3% to 9.8%, and inclusion of illumination losses further reduces the cell efficiency to 7.7% for the slotted-electrode cell.

The maximum power efficiency is presented as a function of illumination intensity in Fig. 10 for the slotted-electrode cell. The cell was designed with the design parameters calculated to be optimal under peak AM-2 illumination. The power efficiency decreases with increasing illumination due to the influence of electrolyte resistance and kinetic and mass-transfer limitations at the counterelectrode. These phenomena become increasingly important as current densities increase, and mass-transfer limitations at the counterelectrode can result in an upper limit for cell currents.



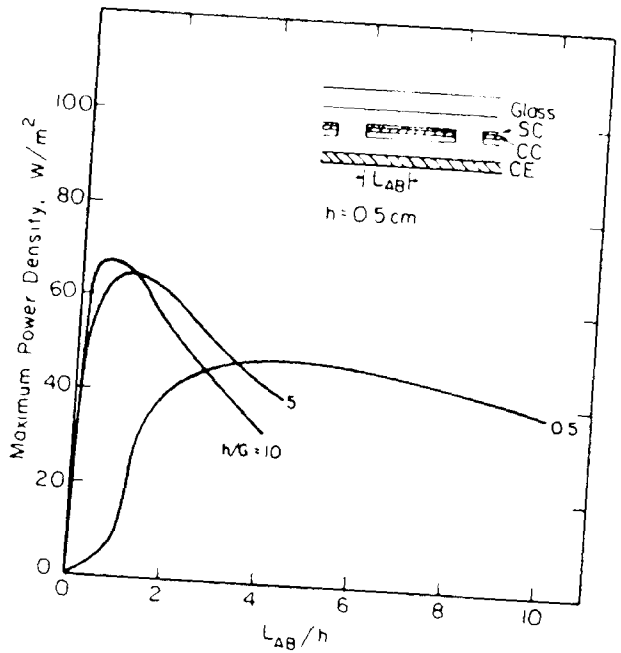


Figure 9. Maximum power density as a function of $L/h$ for the slotted-electrode photoelectrochemical cell (Ref. 211). Reprinted by permission of the publisher, the Electrochemical Society, Inc.

The maximum power efficiency for the system without counterelectrode limitations is also presented in Fig. 10. These results are consistent with the use of a porous counterelectrode in the cell. The maximum cell current obtained under large magnitudes of illumination depends upon the ratio of the counterelectrode area to the semiconductor area. This ratio must be large for liquid-junction photovoltaic cells designed for large intensities of illumination, and for some configurations, a porous counterelectrode may be appropriate.[223] Inclusion of a cooling system in the cell design becomes important under these conditions.[224] The electrolyte itself can serve as a heat exchange in photoelectrochemical systems.

Similar calculations were performed for a cell with a wire-grid counterelectrode through which sunlight passes.[211] Current-potential curves are presented in Fig. 11 for these optimally designed cells as compared to the cell without interfacial kinetic limitations,

**Table 1**
**Power Efficiency under Front Illumination**

| | No illumination losses | Illumination losses[a] | Experimental results[b] |
|---|---|---|---|
| Optimal band gap | 45 | 36 (80%) | |
| GaAs band gap | 37 | 30 (80%) | |
| Semiconductor-electrolyte junction | 15.3 | 12.2 (80%) | 12.0 |
| Slotted-electrode cell design | 9.8 | 7.7 (55.4%) | |

[a] In some cases, the number in parentheses represents the fraction of AM-2 illumination (above the band gap) which actually enters the semiconductor, after accounting for reflection, shadowing, and absorption in intervening phases. In other cases, where detailed calculations were not made, it represents the ratio to column 1 because the nonlinear effect of illumination could not be assessed.
[b] References 28, 91, 92.

counterelectrode limitations, or electrolytic resistance. The cell with a slotted semiconductor has a larger power efficiency than the wire-grid counterelectrode cell and can be designed for separation of chemical products. The analysis of the system designed for separation of chemical products would need to include the electrical resistance of the membrane.

The allowable capital investment for a photovoltaic cell is given by

$$I = 8.76 P_{in} \eta \Delta c y_e \tag{48}$$

where $P_{in}$ is the annual incident illumination intensity averaged over 24 h in $W/m^2$ (on this basis, the average insolation of the continental United States is 200–250 $W/m^2$ [9]), $\eta$ is the cell efficiency, $\Delta c$ is the difference in selling price and operating cost in dollars per kW h, and $y_e$ is the break-even point in years. Lenses or mirrors could be used to increase the amount of sunlight striking the semiconductor surface. Based upon a 7.7% power efficiency (averaged over 24 h), 250 $W/m^2$ incident illumination (averaged over 24 h), \$0.05/kW h profit, and a break-even period of 5 yr, an investment of \$42/$m^2$ is justified for the complete cell. Based upon a 15.3% power efficiency (this number is averaged over 24 h and



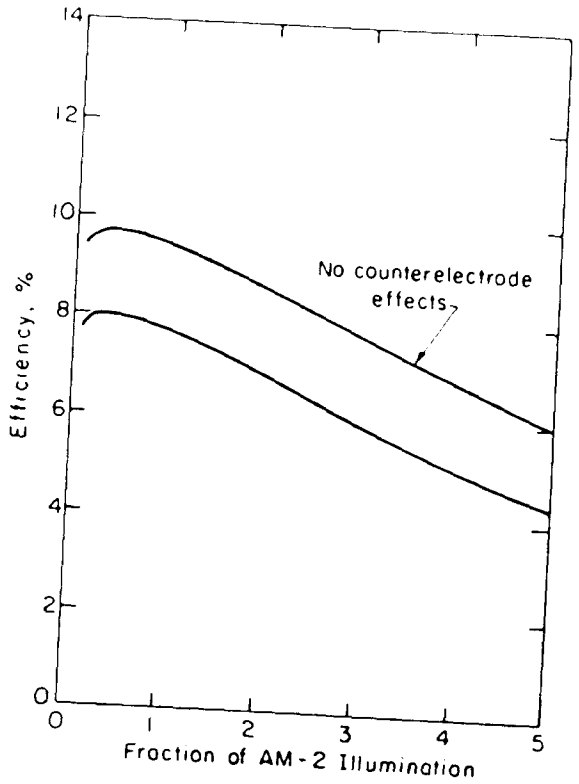


Figure 10. Maximum power efficiency as a function of the fraction of peak Am-2 illumination for a slotted-electrode photoelectrochemical cell with $h/G = 10$ and $L/h = 0.5$ (Ref. 211). Reprinted by permission of the publisher, the Electrochemical Society, Inc.

neglects the influence of cell design), an investment of \$83/$m^2$ is justified for the complete cell.

An increase of solar illumination by a factor of 5 while reducing the efficiency to 6% (see Fig. 10) yields an acceptable initial investment of \$164/$m^2$. If the mirrors and lenses needed to concentrate sunlight are cheaper than the semiconducting film, the cell may be most economical under high illumination. The values presented here can be compared to the cost estimate of \$0.34 per peak watt presented by Weaver *et al.*[225] for a GaAs photoelectrochemical cell. Their estimate is based on materials cost (see also Refs. 226 and

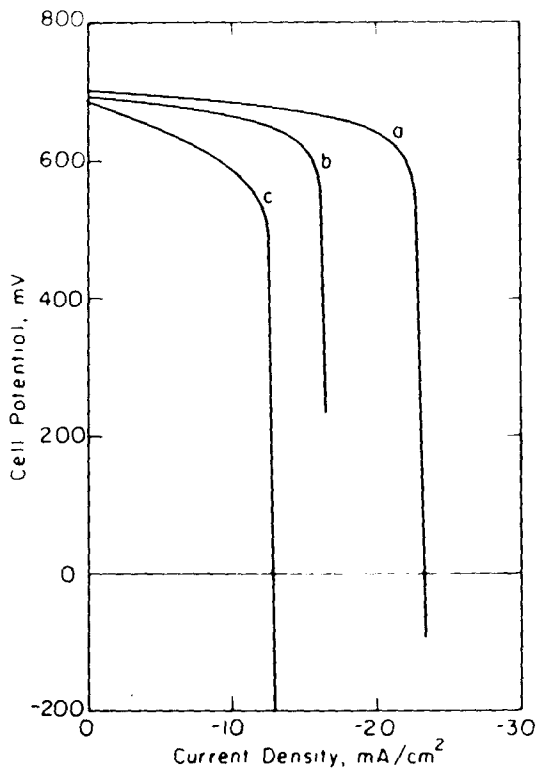


Figure 11. Cell potential as a function of current density for (a) a front-illuminated semiconductor without kinetic, electrolyte resistance, and counterelectrode limitations; (b) an optimally designed slotted-electrode cell with a porous counterelectrode; and (c) an optimally designed cell with a wire-grid counterelectrode of radius 0.5 cm (Ref. 211). Reprinted by permission of the publisher, the Electrochemical Society, Inc.

227) and assumes a cell efficiency of 13%. The influence of cell design was therefore neglected. Under AM-2 illumination, this value corresponds to \$39/m$^2$.

## IV. CONCLUSIONS

Development of a mathematical model of photoelectrochemical devices requires treatment of the diffuse double layer (or space charge region) in the semiconductor. The principles of electrochemical engineering can be readily applied to provide a chemical description of these devices in terms of potentials and concentrations of charged species. The macroscopic transport relations which govern the electrolyte and the semiconductor are coupled by a microscopic model of the interface. Analytic solution of the governing equations requires restrictive assumptions which can be avoided by use of numerical methods.



The optimization of photoelectrochemical devices for solar energy conversion depends on the choice of semiconductor, electrolyte, and cell design. The performance of the cell is strongly dependent upon the design, surface area, and placement of the counterelectrode and current collectors. This type of solar cell may be economical under concentrated illumination or in regions where electrical power has high value.

## ACKNOWLEDGMENT

This work was supported by the Assistant Secretary for Conservation and Renewable Energy, Office of Energy Systems Research, Energy Storage Division of the U. S. Department of Energy, under contract No. DE-AC03-76SF00098.

## NOTATION

### 1. Roman Characters

| | |
|---|---|
| $c_i$ | molar concentration of species $i$ (mol/cm$^3$) |
| $D_i$ | diffusivity of species $i$ (cm$^2$/s) |
| $E_i$ | energy of species or site $i$ (eV) |
| $\Delta E_i$ | ionic adsorption energy (J/mol) |
| $f_i$ | molar activity coefficient of species $i$ |
| $F$ | Faraday's constant (96,487 C/equiv) |
| $G_{th}$ | rate of thermal electron–hole pair generation (mol/s cm$^3$) |
| $G_L$ | rate of photo electron–hole pair generation (mol/s cm$^3$) |
| $i$ | current density (mA/cm$^2$) |
| $i_0$ | exchange current density (mA/cm$^2$) |
| $k_{f,l}$ | forward reaction rate constant for reaction $l$ |
| $k_{b,l}$ | backward reaction rate constant for reaction $l$ |

| | |
|---|---|
| $k_k$ | rate constants for homogeneous reaction $k$ |
| $K_l$ | equilibrium constant for reaction $l$ |
| $m$ | solar absorption coefficient (1/cm) |
| $M_i$ | symbol for chemical formula of species $i$ |
| $n$ | number of electrons involved in electrode reaction |
| $n$ | electron concentration (mol/cm$^3$) |
| $n_i$ | intrinsic electron concentration (mol/cm$^3$) |
| $N$ | total site concentration (mol/cm$^3$) |
| $N_a$ | total bulk electron-acceptor concentration (mol/cm$^3$) |
| $N_d$ | total bulk electron-donor concentration (mol/cm$^3$) |
| $N_i$ | flux of species $i$ (mol/cm$^2$ s) |
| $p$ | hole concentration (mol/cm$^3$) |
| $p_{i,l}$ | heterogeneous reaction order |
| $q_{i,l}$ | heterogeneous reaction order |
| $q_0$ | incident solar flux (mol/s cm$^2$) |
| $r_l$ | heterogeneous reaction rate (mol/s cm$^2$) |
| $R$ | universal gas constant (8.3143 J/mol K) |
| $R_i$ | net rate of production of species $i$ (mol/s cm$^3$) |
| $R_{rec}$ | net rate of electron-hole recombination (mol/s cm$^3$) |
| $s_i$ | stoichiometric coefficient of species $i$ in an electrode reaction |
| $T$ | absolute temperature (K) |
| $u_i$ | mobility of species $i$ (cm$^2$ mol/J s) |
| $V$ | potential drop across depletion layer (V) |
| $W$ | depletion layer thickness (cm) |
| $z_i$ | charge number of species $i$ |

## 2. Greek Characters

| | |
|---|---|
| $\beta$ | symmetry factor |
| $\Gamma_k$ | surface concentration of energy or species $k$ (mol/cm$^2$) |
| $\delta_k$ | distance between interfacial planes (gap denoted by $k$) (cm) |
| $\varepsilon$ | permittivity (C/V cm) |
| $\eta$ | photon efficiency |
| $\eta_k$ | total overpotential at interface $k$ (V) |
| $\Theta$ | fractional occupation of surface sites |
| $\kappa$ | conductivity (mho/cm) |
| $\lambda$ | Debye length (cm) |
| $\mu_i$ | electrochemical potential of species $i$ (J/mol) |
| $\Phi$ | electrical potential (V) |



## 3. Superscripts

| | |
|---|---|
| 0 | equilibrium |
| (-) | secondary reference state at infinite dilution |
| * | secondary reference state in semiconductor |

## 4. Subscripts

| | |
|---|---|
| bulk | associated with the bulk |
| $c$ | associated with conduction band in semiconductor |
| CE | associated with the counterelectrode |
| cell | associated with the cell |
| $e$ | relating to electrons |
| $h$ | relating to holes |
| IHP | associated with inner Helmholtz plane |
| ISS | associated with inner surface states |
| $l$ | associated with reaction $l$ |
| 0 | equilibrium value or initial value |
| OHP | associated with outer Helmholtz plane |
| OSS | associated with outer surface states |
| sc | associated with semiconductor |
| sol | associated with solution |
| $v$ | associated with valence band in semiconductor |

## REFERENCES


[1] A. J. Bard, Photoelectrochemistry and heterogeneous photocatalysis at semiconductors. *J. Photochem.* **10** (1979) 59–75.
[2] A. J. Bard, Photoelectrochemistry, *Science* **207** (1980) 139–144.
[3] A. Fujishima and K. Honda, Electrochemical photolysis of water as a semiconductor electrode, *Nature* **238** (1972) 37–38.
[4] J. Manassen, D. Cahen, and G. Hodes, Electrochemical, solid state, photochemical, and technological aspects of photoelectrochemical energy converters, *Nature* **263** (1976) 97–100.
[5] H. Gerischer and J. Gobrecht, On the power-characteristics of electrochemical solar cells, *Ber. Bunsenges. Phys. Chem.* **80** (1976) 327–330.
[6] H. Ehrenreich and J. H. Martin, Solar photovoltaic energy, *Phys. Today* **32**(9) (1979) 25–32.
[7] H. Gerischer, Heterogeneous electrochemical systems for solar energy conversion, *Pure Appl. Chem.* **52** (1980) 2649–2667.
[8] A. Heller, Electrochemical solar cells, *Solar Energy* **29** (1982) 153–162.

[9] M. Green, Electrochemistry of the semiconductor electrolyte interface, Chap. 5 in *Modern Aspects of Electrochemistry*, No. 2, Ed. by J. O'M. Bockris, Academic, New York, 1959.
[10] H. Gerischer, Semiconductor electrode reactions, Chap. 4 in *Advances in Electrochemistry and Electrochemical Engineering*, Vol. 1, Ed. by P. Delahay, Interscience, New York, 1961.
[11] M. D. Archer, Electrochemical aspects of solar energy conversion, *J. Appl. Electrochem.* **5** (1975) 17-38.
[12] K. Rajeshwar, P. Singh, and J. DuBow, Energy conversion in photoelectrochemical systems: A review, *Electrochim. Acta* **23** (1975) 1117-1144.
[13] L. A. Harris and R. H. Wilson, Semiconductors for photoelectrolysis, *Ann. Rev. Mater. Sci.* **8** (1978) 99-134.
[14] A. J. Nozik, Photoelectrochemistry: Applications to solar energy conversion, *Ann. Rev. Phys. Chem.* **29** (1978) 189-222.
[15] M. Tomkiewicz and H. Fay, Photoelectrolysis of water with semiconductors, *Appl. Phys.* **18** (1979) 1-28.
[16] R. H. Wilson, Electron transfer processes at the semiconductor-electrolyte interface, *CRC Crit. Rev. Solid State Mater. Sci.* **10** (1980) 1-41.
[17] R. Memming, Charge transfer processes at semiconductor electrodes, in *Electroanalytical Chemistry*, Ed. by Allen J. Bard, Marcel Dekker, New York, 1981, pp. 1-84.
[18] S. R. Morrison, *Electrochemistry at Semiconductor and Oxidized Metal Electrodes*, Plenum Press, New York, 1980.
[19] U. M. Khan and J. O'M Bockris, Photoelectrochemical kinetics and related devices, Chap. 3 in *Modern Aspects of Electrochemistry*, No. 14, Ed. by J. O'M. Bockris, B. E. Conway, and R. E. White, Plenum Press, New York, 1982.
[20] A. S. Grove, *Physics and Technology of Semiconductor Devices*, Wiley, New York, 1967.
[21] M. A. Omar, *Elementary Solid State Physics: Principles and Applications*, Addison-Wesley, Menlo Park, California, 1975.
[22] S. M. Sze, *Physics of Semiconductor Devices*, Wiley-Interscience, New York, 1969.
[23] N. B. Hannay, Semiconductor principles, Chap. 1 in *Semiconductors*, Ed. by N. B. Hannay, Reinhold, New York, 1959.
[24] A. F. Ioffe, *Physics of Semiconductors*, Academic, New York, 1960.
[25] J. Hovel, Solar cells, Vol. 11 of *Semiconductors and Semimetals*, Ed. by R. K. Willardson and Albert C. Beer, Academic, New York, 1975.
[26] H. J. Hovel, Photovoltaic materials and devices for terrestrial solar energy applications, *Solar Energy Mater.* **2** (1980) 277-312.
[27] S. Wagner, Physico-chemical problems in photovoltaic research, *Ber. Bunsenges. Phys. Chem.* **84** (1980) 991-995.
[28] A. Heller, Conversion of sunlight into electrical power and photoassisted electrolysis of water in photoelectrochemical cells, *Acc. Chem. Res.* **14** (1981) 154-162.
[29] K. W. Mitchell, Status of new thin-film photovoltaic technologies, *Ann. Rev. Mater. Sci.* **12** (1982) 401-415.
[30] D. C. Grahame, The electrical double layer and the theory of electrocapillarity, *Chem. Rev.* **41** (1947) 441-501.
[31] J. F. Dewald, Semiconductor electrodes, Chap. 17 in *Semiconductors*, Ed. by N. B. Hannay, Reinhold, New York, 1959.
[32] M. J. Sparnaay, *The Electrical Double Layer*, Pergamon, New York, 1972.
[33] J. Newman, *Electrochemical Systems*, Prentice-Hall, Englewood Cliffs, New Jersey, 1973.
[34] S. J. Fonash, *Solar Cell Device Physics*, Academic, New York, 1981.



[35] M. E. Orazem, *Mathematical modeling and optimization of liquid-junction photovoltaic cells*, Ph.D. dissertation, Department of Chemical Engineering, University of California, Berkeley, June 1983, LBL-16131.
[36] M. E. Orazem and J. Newman, Mathematical modeling of liquid-junction photovoltaic cells: I. Governing equations, *J. Electrochem. Soc.* **131** (1984) 2569-2574.
[37] M. E. Orazem and J. Newman, Mathematical modeling of liquid-junction photovoltaic cells: II. Effect of system parameters on current-potential curves, *J. Electrochem. Soc.* **131** (1984) 2574-2582.
[38] E. A. Guggenheim, The conceptions of electrical potential difference between two phases and the individual activities of ions, *J. Phys. Chem.* **33** (1929) 842-849.
[39] R. Memming, Solar energy conversion by photoelectrochemical processes, *Electrochim. Acta* **25** (1980) 77-88.
[40] R. Parsons, Equilibrium properties of electrified interphases, Chap. 3 in *Modern Aspects of Electrochemistry*, No. 1, Ed. by J. O'M. Bockris, Academic, New York, 1954, pp. 103-179.
[41] A. J. Rosenberg, Activity coefficients of electrons and holes at high concentrations, *J. Chem. Phys.* **33** (1960) 655-667.
[42] W. W. Harvey, The relation between the chemical potential of electrons and energy band parameters of the band theory as applied to semiconductors, *J. Phys. Chem. Solids* **23** (1962) 1545-1548.
[43] P. T. Landsberg and A. G. Guy, Activity coefficient and the Einstein relation, *Phys. Rev. B: Condensed Matter* **28** (1983) 1187-1188.
[44] M. B. Panish and H. C. Casey, Jr., The solid solubility limits of zinc in GaAs at 1000°, *J. Phys. Chem. Solids* **28** (1967) 1673-1684.
[45] M. B. Panish and H. C. Casey, Jr., The 1040° solid solubility isotherm of zinc in GaP: the Fermi level as a function of hole concentration, *J. Phys. Chem. Solids* **28** (1968) 1719-1726.
[46] J. C. Hwang and J. R. Brews, Electron activity coefficients in heavily doped semiconductors with small effective mass, *J. Phys. Chem. Solids* **32** (1971) 837-845.
[47] N. G. Nilsson, Empirical approximation for the Fermi energy in a semiconductor with parabolic bands, *Appl. Phys. Lett.* **33** (1978) 653-654.
[48] J. S. Blakemore, Approximations for Fermi-Dirac integrals, especially of order 1/2 used to describe electron density in a semiconductor, *Solid State Electron.* **25** (1982) 1067-1076.
[49] X. Aymerich-Humet, F. Serra-Mestres, and J. Millan, An analytical approximation for the Fermi-Dirac integral $F_{1/2}(\eta)$, *Solid State Electron.* **24** (1981) 981-982.
[50] M. A. Shibib, Inclusion of degeneracy in the analysis of heavily doped regions in silicon solar cells and other semiconductor devices, *Solar Cells* **3** (1981) 81-85.
[51] H. P. D. Lanyon, The physics of heavily doped $n^+$-$p$ junction solar cells, *Solar Cells* **3** (1981) 289-311.
[52] S. R. Dhariwal and V. N. Ojha, Band gap narrowing in heavily doped silicon, *Solid State Electron.* **25** (1982) 909-911.
[53] F. A. Lindholm and J. G. Fossum, Pictorial derivation of the influence of degeneracy and disorder on nondegenerate minority-carrier concentration and recombination current in heavily doped silicon, *IEEE Electron Device Lett.* **EDL-2** (1981) 230-234.
[54] R. A. Abram, G. J. Rees, and B. L. H. Wilson, Heavily doped semiconductor devices, *Adv. Phys.* **27** (1978) 799-892.
[55] G. D. Mahan, Energy gap in Si and Ge: Impurity dependence, *J. Appl. Phys.* **51** (1980) 2634-2646.

[56] D. S. Lee and J. G. Fossum, Energy band distortion in highly doped silicon, *IEEE Trans. Electron Devices* **ED-30** (1983) 626–634.
[57] S. Selberherr, *Analysis and Simulation of Semiconductor Devices*, Springer-Verlag, New York, 1984.
[58] M. E. Orazem and J. Newman, Activity coefficients of electrons and holes in semiconductors, *J. Electrochem. Soc.* **131** (1984) 2715–2717.
[59] D. B. Bonham and M. E. Orazem, Activity coefficients of electrons and holes in semiconductors with a parabolic density of states, *J. Electrochem. Soc.* (in press).
[60] A. G. Guy, Calculation of activity coefficients of conduction electrons in metals and semiconductors, *Solid State Electron.* **26** (1983) 433–436.
[61] P. T. Landsberg and S. A. Hope, Two formulations of semiconductor transport equations, *Solid State Electron.* **20** (1977) 421–429.
[62] M. S. Lundstrom, R. J. Schwartz, and J. L. Gray, Transport equations for the analysis of heavily doped semiconductor devices, *Solid State Electron.* **24** (1981) 195–202.
[63] A. H. Marshak and R. Shrivastava, Calculation of the electric field enhancement for a degenerate diffusion process, *Solid State Electron.* **25** 151–153.
[64] D. Kumar and S. K. Sharma, Theory of open circuit photo-voltage in degenerate abrupt $p$–$n$ junctions, *Solid State Electron.* **25** (1982) 1161–1164.
[65] P. T. Landsberg, *Thermodynamics and Statistical Mechanics*, Oxford University Press, New York, 1978, p. 327.
[66] R. B. Bird, W. E. Stewart, and E. N. Lightfoot, *Transport Phenomena*, Wiley, New York, 1960.
[67] R. A. Smith, *Semiconductors*, Cambridge University Press, London, 1959.
[68] R. G. Shulman, Recombination and trapping, Chap. 11 in *Semiconductors*, Ed. by N. B. Hannay, Reinhold, New York, 1959.
[69] J. L. Moll, *Physics of Semiconductors*, McGraw-Hill, New York, 1964.
[70] H. Gerischer, Semiconductor electrochemistry, Chap. 5 in *Physical Chemistry: An Advanced Treatise*, Vol. IX, Ed. by H. Eyring, Academic, New York, 1970.
[71] P. Delahay, *Double Layer and Electrode Kinetics*, Interscience, New York, 1965.
[72] H. Oman and J. W. Gelzer, Solar cells and arrays, in *Energy Technology Handbook*, Ed. by Douglas M. Considine, McGraw-Hill, New York, 1977, pp. 6.56–6.80.
[73] M. A. Russak, J. Reichman, H. Witzke, S. K. Deb, and S. N. Chen, Thin film CdSe photoanodes for electrochemical photovoltaic solar cells, *J. Electrochem. Soc.* **127** (1980) 725–733.
[74] M. S. Kazacos and B. Miller, Electrodeposition of CdSe films from selenosulfite solution, *J. Electrochem. Soc.* **127** (1980) 2378–2381.
[75] C.-H. J. Liu, J. Olsen, D. R. Saunders, and J. H. Wang, Photoactivation of CdSe films for photoelectrochemical cells, *J. Electrochem. Soc.* **128** (1981) 1224–1228.
[76] C.-H. J. Liu and J. H. Wang, Spray-pyrolyzed thin film CdSe photoelectrochemical cells, *J. Electrochem. Soc.* **129** (1982) 719–722.
[77] D. R. Pratt, M. E. Langmuir, R. A. Boudreau, and R. D. Rauh, Chemically deposited CdSe thin films for photoelectrochemical cells, *J. Electrochem. Soc.* **128** (1981) 1627–1629.
[78] K. Rajeshwar, L. Thompson, P. Singh, R. C. Kainthla, and K. L. Chopra, Photoelectrochemical characterization of CdSe thin film anodes, *J. Electrochem. Soc.* **128** (1981) 1744–1750.
[79] J. Reichman and M. A. Russak, Properties of CdSe thin films for photoelectrochemical cells, *J. Electrochem. Soc.* **128** (1981) 2025–2029.



[80] J. Reichman and M. A. Russak, Improved efficiency of $n$-CdSe thin-film photo electrodes by zinc surface treatment, *J. Appl. Phys.* **53** (1982) 708–711.
[81] G. J. Houston, J. F. McCann, and D. Haneman, Optimizing the photoelectrochemical performance of electrodeposited CdSe semiconductor electrodes, *J. Electroanal. Chem.* **134** (1982) 37–47.
[82] B. Miller, A. Heller, M. Robbins, S. Menezes, K. C. Chang, and J. Thomson, Jr., Solar conversion efficiency of pressure-sintered cadmium selenide liquid-junction cells, *J. Electrochem. Soc.* **124** (1977) 1019–1021.
[83] A. Heller, K. C. Chang, and B. Miller, Spectral response and efficiency relations in semiconductor liquid junction solar cells, *J. Electrochem. Soc.* **124** (1977) 697–700.
[84] B. Miller and A. Heller, Semiconductor liquid junction solar cells based on anodic sulphide films, *Nature* **262** (1976) 680–681.
[85] L. M. Peter, The photoelectrochemical properties of anodic cadmium sulphide films, *Electrochim. Acta* **23** (1978) 1073–1080.
[86] C. C. Tsou and J. R. Cleveland, Polycrystalline thin-film CdSe liquid junction photovoltaic cell, *J. Appl. Phys.* **51** (1980) 455–458.
[87] R. A. L. Vanden Berghe, W. P. Gomes, and F. Cardon, Some aspects of the anodic behavior of CdS single crystals in indifferent electrolyte solutions, *Ber. Bunsenges. Phys. Chem.* **77** (1973) 289–293.
[88] A. Heller, B. Miller, S. S. Chu, and Y. T. Lee, 7.3% efficient thin-film, polycrystalline $n$-GaAs semiconductor liquid junction solar cell, *J. Am. Chem. Soc.* **101** (1979) 7633–7634.
[89] W. D. Johnston, Jr., H. J. Leamy, B. A. Parkinson, A. Heller, and B. Miller, Effect of ruthenium ions on grain boundaries in gallium arsenide thin film photovoltaic devices, *J. Electrochem. Soc.* **127** (1980) 90–95.
[90] R. Noufi and D. Tench, High efficiency GaAs photoanodes, *J. Electrochem. Soc.* **127** (1980) 188–190.
[91] A. Heller and B. Miller, Photoelectrochemical solar cells: Chemistry of the semiconductor–liquid junction, Chap. 12 in *Interfacial Photoprocesses: Energy Conversion and Synthesis*, Advances in Chemistry Series, 184, Ed. by M. S. Wrighton, American Chemical Society, Washington, D.C., 1980.
[92] B. A. Parkinson, A. Heller, and B. Miller, Enhanced photoeletrochemical solar-energy conversion by gallium-arsenide surface modification, *Appl. Phys. Lett.* **33** (1978) 521–523.
[93] J. Belloni, G. Van Amerongen, M. Herlem, J.-L. Sculfort, and R. Heindl, Photocurrents from semiconductor–liquid ammonia junctions, *J. Phys. Chem.* **84** (1980) 1269–1270.
[94] M. A. Butler, R. D. Nasby, and R. K. Quinn, Tungsten trioxide as an electrode for photoelectrolysis of water, *Solid State Commun.* **19** (1976) 1011–1014.
[95] M. P. Dare-Edwards, A. Hamnett, and J. B. Goodenough, The efficiency of photogeneration of hydrogen at $p$-type III/V semiconductors, *J. Electroanal. Chem.* **119** (1981) 109–123.
[96] A. B. Ellis, S. W. Kaiser, and M. S. Wrighton, Semiconducting potassium tantalate electrodes. Photoassistance agents for the efficient electrolysis of water, *J. Phys. Chem.* **80** (1976) 1325–1328.
[97] F.-R. F. Fan, H. S. White, R. Wheeler, and A. J. Bard, Semiconductor electrodes: XXIX. High efficiency photoelectrochemical solar cells with $n$-$WSe_2$ electrodes in an aqueous iodide medium, *J. Electrochem. Soc.* **127** (1980) 518–520.
[98] W. Gissler, P. L. Lensi, and S. Pizzini, Electrochemical investigation of an illuminated $TiO_2$ electrode, *J. Appl. Electrochem.* **6** (1976) 9–13.

[99] J. Gobrecht, R. Potter, R. Nottenburg, and S. Wagner, An *n*-CdSe/$SnO_2$/*n*-Si tandem electrochemical solar cell, *J. Electrochem. Soc.* **130** (1983) 2280–2283.
[100] K. Hirano and A. J. Bard, Semiconductor electrodes: XXVIII. Rotating ring-disk electrode studies of photo-oxidation of acetate and iodide at *n*-$TiO_2$, *J. Electrochem. Soc.* **127** (1980) 1056–1059.
[101] P. A. Kohl and A. J. Bard, Semiconductor electrodes: XVII. Electrochemical behavior of *n*- and *p*-type InP electrodes in acetonitrile solutions, *J. Electrochem. Soc.* **126** (1979) 598–608.
[102] H. H. Kung, H. S. Jarrett, A. W. Sleight, and A. Ferretti, Semiconducting oxide anodes in photoassisted electrolysis of water, *J. Appl. Phys.* **48** (1977) 2463–2469.
[103] Y. Nakato, N. Takamori, and H. Tsubomura, A composite semiconductor photoanode for water electrolysis, *Nature* **295** (1982) 312–313.
[104] K. Uosaki and H. Kita, Photoelectrochemical characteristics of semiconductor-metal/SPE/metal cells, *J. Electrochem. Soc.* **130** (1983) 2179–2184.
[105] D. Cahen, J. Manassen, and G. Hodes, Materials aspect of photoelectrochemical systems, *Solar Energy Mater.* **1** (1979) 343–355.
[106] A. W. Czanderna, Stability of interfaces in solar energy materials, *Solar Energy Mater.* **5** (1981) 349–377.
[107] L. E. Murr, Interfacial phenomena in solar materials, *Solar Energy Mater.* **5** (1981) 1–19.
[108] J. J. Loferski, Theoretical considerations governing the choice of the optimum semiconductor for photovoltaic solar energy conversion, *J. Appl. Phys.* **27** (1956) 777–784.
[109] J. J. Loferski, Recent research on photovoltaic solar energy converters, *Proc. IEEE* **51** (1963) 667–674.
[110] J. J. Wysocki, Photon spectrum outside the earth's atmosphere, *Solar Energy* **6** (1962) 104.
[111] M. Wolf, Limitations and possibilities for improvement of photovoltaic solar energy converters, Part I: Considerations for earth's surface operation, *Proc. IRE* **48** (1960) 1246–1263.
[112] W. Shockley and H. J. Queisser, Detailed balance limit of efficiency of *p*–*n* junction solar cells, *J. Appl. Phys.* **32** (1961) 510–519.
[113] K. C. Chang, A. Heller, B. Schwartz, S. Menezes, and B. Miller, Stable semiconductor liquid-junction cell with 9% solar to electrical conversion efficiency, *Science* **196** (1977) 1097–1098.
[114] A. B. Ellis, J. M. Bolts, S. W. Kaiser, and M. S. Wrighton, Study of *n*-type gallium arsenide- and gallium phosphide-based photoelectrochemical cells. Stabilization by kinetic control and conversion of optical energy to electricity, *J. Am. Chem. Soc.* **99** (1977) 2848–2854.
[115] P. Josseaux, A. Kirsch-De Mesmaeker, J. Riga, and J. Verbist, Improvements of CdS film photoanodic behavior by sulfur organic reducing agents, *J. Electrochem. Soc.* **130** (1983) 1067–1074.
[116] M. S. Wrighton, J. M. Bolts, A. B. Bocarsly, M. C. Palazzotto, and E. G. Walton, Stabilization of *n*-type semiconductors to photoanodic dissolution: II-VI and III-V compound semiconductors and recent results for *n*-type silicon, *J. Vac. Sci. Technol.* **15** (1978) 1429–1435.
[117] A. Heller, B. Miller, and F. A. Thiel, 11.5% Solar conversion efficiency in the photocathodically protected *p*-InP/$V^{3+}$-$V^{2+}$-HCl semiconductor liquid-junction cell, *Appl. Phys. Lett.* **38** (1981) 282–284.
[118] D. S. Ginley, R. J. Baughman, and M. A. Butler, BP-Stabilized *n*-Si and *n*-GaAs photoanodes, *J. Electrochem. Soc.* **130** (1983) 1999–2002.



[119] H. Gerischer, Photoelectrochemical solar cells, in *Proceedings of the 2nd Electrochemical Photovoltaic Solar Energy Conference*, Ed. by R. van Overstraeten and W. Palz, Reidel, Boston, 1979, pp. 408–431.
[120] S. Menezes, A. Heller, and B. Miller, Metal filmed-semiconductor photoelectrochemical cells, *J. Electrochem. Soc.* **127** (1980) 1268–1273.
[121] K. W. Frese, Jr., M. J. Madou, and S. R. Morrison, Investigation of photoelectrochemical corrosion of semiconductors: III. Effects of metal layers on the stability of GaAs, *J. Electrochem. Soc.* **128** (1981) 1939–1943.
[122] R. Noufi, D. Tench, and L. F. Warren, Protection of *n*-GaAs photoanodes with photoelectrochemically generated polypyrrole films, *J. Electrochem. Soc.* **127** (1980) 2310–2311.
[123] R. Noufi, D. Tench, and L. F. Warren, Protection of semiconductor photoanodes with photoelectrochemically generated polypyrrole films, *J. Electrochem. Soc.* **128** (1981) 2596–2599.
[124] T. Skotheim, I. Lundstrom, and J. Prejza, Stabilization of *n*-Si photoanodes to surface corrosion in aqueous electrolyte with a thin film of polypyrrole, *J. Electrochem. Soc.* **128** (1981) 1625–1626.
[125] T. Skotheim, L.-G. Petersson, O. Inganas, and I. Lundstrom, Photoelectrochemical behavior of *n*-Si electrodes protected with Pt-polypyrrole, *J. Electrochem. Soc.* **129** (1982) 1737–1741.
[126] F.-R. F. Fan, R. L. Wheeler, A. J. Bard, and R. N. Noufi, Semiconductor electrodes XXXIX. Techniques for stabilization of *n*-silicon electrodes in aqueous solution photoelectrochemical cells, *J. Electrochem. Soc.* **128** (1981) 2042–2045.
[127] R. A. Bull, F.-R. F. Fan and A. J. Bard, Polymer films on electrodes VII. Electrochemical behavior at polypyrrole-coated platinum and tantalum electrodes, *J. Electrochem. Soc.* **129** (1982) 1009–1015.
[128] K. Rajeshwar, M. Kaneko, and A. Yamada, Regenerative photoelectrochemical cells using polymer-coated *n*-GaAs photoanodes in contact with aqueous electrolytes, *J. Electrochem. Soc.* **130** (1983) 38–43.
[129] H. S. White, H. D. Abruna, and A. J. Bard, Semiconductor electrodes XLI. Improvement of performance of *n*-$WSe_2$ electrodes by electrochemical polymerization of *o*-phenylenediamine at surface imperfections, *J. Electrochem. Soc.* **129** (1982) 265–271.
[130] L. Fornarini, F. Stirpe, and B. Scrosati, Electrochemical solar cells with layer-type semiconductor anodes: Stabilization of the semiconductor electrode by selective polyindole electrodeposition, *J. Electrochem. Soc.* **130** (1983) 2184–2187.
[131] M. S. Wrighton, Photoelectrochemical conversion of optical energy to electricity and fuels, *Acc. Chem. Res.* **12** (1979) 303–310.
[132] H. Gerischer, On the stability of semiconductor electrodes against photodecomposition, *J. Electroanal. Chem.* **82** (1977) 133–143.
[133] G. L. Araujo, and E. Sanchez, Analytical expressions for the determination of the maximum power point and the fill factor of a solar cell, *Solar Cells* **5** (1982) 377–386.
[134] J. P. Charles, M. Zaghdoudi, P. Mialhe, and A. Marrakchi, An analytical model for solar cells, *Solar Cells* **3** (1981) 45–56.
[135] J. P. Charles, M. Abdelkrim, Y. H. Muoy, and P. Mialhe, A practical method of analysis of the current-voltage characteristics of solar cells, *Solar Cells* **4** (1981) 169–178.
[136] A. De Vos, The fill factor of a solar cell from a mathematical point of view, *Solar Cells* **8** (1983) 283–296.

[137] G. S. Kousik and J. G. Fossum, $P^+$-$N$-$N^+$ Solar cells with hole diffusion lengths comparable with the base width: A simple analytic model, *Solar Cells* **5** (1981-1982) 75-79.
[138] W. A. Miller and L. C. Olsen, Model calculations for silicon inversion layer solar cells, *Solar Cells* **8** (1983) 371-395.
[139] P. Panayotatos and H. C. Card, Recombination in the space-charge region of Schottky barrier solar cells, *Solid State Electron.* **23** (1980) 41-47.
[140] C. M. Singal, Analytical expressions for the series-resistance-dependent maximum power point and curve factor for solar cells, *Solar Cells* **3** (1981) 163-177.
[141] E. J. Soukup and D. R. Slocum, A model for the collection of minority carriers generated in the depletion region of a Schottky barrier solar cell, *Solar Cells* **7** (1982-1983) 297-310.
[142] G. P. Srivastava, P. K. Bhatnagar, and S. R. Dhariwal, Theory of metal-oxide-semiconductor solar cells, *Solid State Electron.* **22** (1979) 581-587.
[143] N. G. Tarr and D. L. Pulfrey, An investigation of dark current and photocurrent superposition in photovoltaic devices, *Solid State Electron.* **22** (1979) 265-270.
[144] R. Tenne, N. Muller, Y. Mirovsky, and D. Lando, The relation between performance and stability of Cd-chalcogenide/polysulfide photoelectrochemical cells: I. Model and the effect of photoetching, *J. Electrochem. Soc.* **130** (1983) 852-860.
[145] K. M. Van Vliet and A. H. Marshak, The Schottky-like equations for the carrier densities and the current flows in materials with a nonuniform composition, *Solid State Electron.* **23** (1980) 49-53.
[146] W. W. Gärtner, Depletion-layer photoeffects in semiconductors, *Phys. Rev.* **116** (1959) 84-87.
[147] M. A. Butler, Photoelectrolysis and physical properties of the semiconducting electrode $WO_3$, *J. Appl. Phys.* **48** (1977) 1914-1920.
[148] W. Kautek, H. Gerischer, and H. Tributsch, The role of carrier diffusion and indirect optical transitions in the photoelectrochemical behavior of layer type *d*-band semiconductors, *J. Electrochem. Soc.* **127** (1980) 2471-2478.
[149] L. McC. Williams, *Structural and photoelectrochemical properties of plasma deposited titanium dioxide*, Ph.D. thesis, University of California, Berkeley, December, 1982, LBL-14994.
[150] R. H. Wilson, A model for the current-voltage curve of photoexcited semiconductor electrodes, *J. Appl. Phys.* **48** (1977) 4292-4297.
[151] R. H. Wilson, A model for the current-voltage curve of photoexcited semiconductor electrodes, in *Semiconductor Liquid-Junction Solar Cells*, Ed. by A. Heller, The Electrochemical Society, Princeton, New Jersey, 1977.
[152] W. J. Albery, P. N. Bartlett, A. Hamnett, and M. P. Dare-Edwards, The transport and kinetics of minority carriers in illuminated semiconductor electrodes, *J. Electrochem. Soc.* **128** (1981) 1492-1501.
[153] W. J. Albery and P. N. Bartlett, The recombination of photogenerated minority carriers in the depletion layer of semiconductor electrodes, *J. Electrochem. Soc.* **130** (1983) 1699-1706.
[154] W. J. Albery and P. N. Bartlett, The transport and kinetics of photogenerated carriers in colloidal semiconductor electrode particles, *J. Electrochem. Soc.* **131** (1984) 315-325.
[155] J. Reichman, The current-voltage characteristics of semiconductor-electrolyte junction photovoltaic cells, *Appl. Phys. Lett.* **36** (1980) 574-577.
[156] J. Reichman, Collection efficiency of low-mobility solar cells, *Appl. Phys. Lett.* **38** (1981) 251-253.



[157] H. Reiss, Photocharacteristics for electrolyte-semiconductor junctions, *J. Electrochem. Soc.* **125** (1978) 937-949.
[158] W. L. Ahlgren, Analysis of the current-voltage characteristics of photoelectrolysis cells, *J. Electrochem. Soc.* **128** (1981) 2123-2128.
[159] J. F. McCann and D. Haneman, Recombination effects on current-voltage characteristics of illuminated surface barrier cells, *J. Electrochem. Soc.* **129** (1982) 1134-1145.
[160] J. F. McCann, S. Hinckley, and D. Haneman, An analysis of the current-voltage characteristics of thin-film front wall illuminated and back wall illuminated liquid junction and Schottky barrier solar cells, *J. Electrochem. Chem.* **137** (1982) 17-37.
[161] K. E. Heusler and M. Schulze, Electron-transfer reactions at semiconducting anodic niobium oxide films, *Electrochim. Acta* **20** (1975) 237-244.
[162] F. Williams and A. J. Nozik, Irreversibilities in the mechanism of photoelectrolysis, *Nature* **271** (1978) 137-139.
[163] R. H. Wilson, Observation and analysis of surface states on TiO electrodes in aqueous electrolytes, *J. Electrochem. Soc.* **127** (1980) 228-234.
[164] S. M. Ahmed and H. Gerischer, Influence of crystal surface orientation on redox reactions at semiconducting $MoS_2$, *Electrochim. Acta* **24** (1979) 705-711.
[165] A. Aruchamy and M. S. Wrighton, A comparison of the interface energetics for *n*-type cadmium sulfide- and cadmium telluride-nonaqueous electrolyte junctions, *J. Phys. Chem.* **84** (1980) 2848-2854.
[166] A. J. Bard, A. B. Bocarsly, F.-R. F. Fan, E. G. Walton, and M. S. Wrighton, The concept of Fermi level planning at semiconductor-liquid junctions. Consequences for energy conversion efficiency and selection of useful solution redox couples in solar devices, *J. Am. Chem. Soc.* **102** (1980) 3671-3677.
[167] F.-R. F. Fan and A. J. Bard, Semiconductor electrodes. 24. Behavior and photoelectrochemical cells based on *p*-type GaAs in aqueous solutions, *J. Am. Chem. Soc.* **102** (1980) 3677-3683.
[168] A. B. Bocarsly, D. C. Bookbinder, R. N. Dominey, N. S. Lewis, and M. S. Wrighton, Photoreduction at illuminated *p*-type semiconducting silicon photoelectrodes. Evidence for Fermi level pinning, *J. Am. Chem. Soc.* **102** (1980) 3683-3688.
[169] G. Nagasubramanian, B. L. Wheeler, and A. J. Bard, Semiconductor electrodes: XLIX. Evidence for Fermi level pinning and surface-state distributions from impedence measurements in acetonitrile solutions with various redox couples, *J. Electrochem. Soc.* **130** (1983) 1680-1688.
[170] D. C. Card and H. C. Card, Interfacial oxide layer mechanisms in the generation of electricity and hydrogen by solar photoelectrochemical cells, *Solar Energy* **28** (1982) 451-460.
[171] R. Haak and D. Tench, Electrochemical photocapacitance spectroscopy method for characterization of deep levels and interface states in semiconductor materials, *J. Electrochem. Soc.* **131** (1984) 275-283.
[172] W. Siripala and M. Tomkiewicz, Surface recombination at *n*-$TiO_2$ electrodes in photoelectrolytic solar cells, *J. Electrochem. Soc.* **130** (1983) 1062-1067.
[173] K. Uosaki and H. Kita, Effects of the Helmholtz layer capacitance on the potential distribution at semiconductor/electrolyte interface and the linearity of the Mott-Schottky plot, *J. Electrochem. Soc.* **130** (1983) 895-897.
[174] C. G. B. Garrett and W. H. Brattain, Physical theory of semiconductor surfaces, *Phys. Rev.* **99** (1955) 376-387.
[175] E. O. Johnson, Large-signal surface photovoltage studies with germanium, *Phys. Rev.* **111** (1958) 153-166.

[176] A. Many, Y. Goldstein and N. B. Grover, *Semiconductor Surfaces*, North-Holland, Amsterdam, 1965.
[177] S. R. Morrison, *The Chemical Physics of Surfaces*, Plenum Press, New York, 1977.
[178] J. O'M. Bockris and K. Uosaki, The theory of the light-induced evolution of hydrogen at semiconductor electrodes, *J. Electrochem. Soc.* **125** (1978) 223-227.
[179] R. Memming, The role of energy levels in semiconductor-electrolyte solar cells, *J. Electrochem. Soc.* **125** (1978) 117-123.
[180] K. W. Frese, Jr., A study of rearrangement energies of redox species, *J. Phys. Chem.* **85** (1981) 3911-3916.
[181] W. Kautek and H. Gerischer, A kinetic derivation of the photovoltage for electrochemical solar cells employing small-band gap semiconductors, *Electrochim. Acta* **27** (1982) 355-358.
[182] K. Rajeshwar, Charge transfer in photoelectrochemical devices via interface states: United model and comparison with experimental data, *J. Electrochem. Soc.* **129** (1982) 1003-1008.
[183] J.-N. Chazalviel, Electrochemical transfer via surface states: A new formulation for the semiconductor-electrolyte interface, *J. Electrochem. Soc.* **129** (1982) 963-969.
[184] P. Singh, K. Rajeshwar, R. Singh, and J. DuBow, Estimation of series resistance losses and ideal fill factors for photoelectrochemical cells, *J. Electrochem. Soc.* **128** (1981) 1396-1398.
[185] J. F. McCann, S. P. S. Badwal, and J. Pezy, The electrical analogue of an $n$-$SnO_2$-1 M NaOH-Pt cell, *J. Electroanal. Chem.* **118** (1981) 115-130.
[186] J. F. McCann and S. P. S. Badwal, Equivalent circuit analysis of the impedance response of semiconductor-electrolyte-counterelectrode cells, *J. Electrochem. Soc.* **129** (1982) 551-559.
[187] J. R. Macdonald, Accurate solution of an idealized one-carrier metal-semiconductor junction problem, *Solid-State Electron.* **5** (1962) 11-37.
[188] A. De Mari, An accurate numerical steady-state one-dimensional solution of the $p$-$n$ junction, *Solid-State Electron.* **11** (1968) 33-58.
[189] A. De Mari, An accurate numerical steady-state one-dimensional solution of the $p$-$n$ junction under arbitrary transient conditions, *Solid-State Electron.* **11** (1968) 1021-1053.
[190] S. C. Choo, Numerical analysis of a forward-biased step-junction $p$-$i$-$n$ diode, *IEEE Trans. Electron Devices* **ED-18** (1971) 574-586.
[191] S. C. Choo, Theory of a forward-biased diffused-junction $p$-$i$-$n$ rectifier—Part 1: Exact numerical solution, *IEEE Trans. Electron Devices* **ED-19** (1972) 954-966.
[192] J. E. Sutherland and J. R. Hauser, A computer analysis of heterojunction and graded composition solar cells, *IEEE Trans. Electron Devices* **ED-24** (1977) 363-372.
[193] M. Hack and M. Shur, Computer simulation of amorphous silicon based $p$-$i$-$n$ solar cells, *IEEE Electron Device Lett.* **EDL-4** (1983) 140-143.
[194] M. F. Lamorte and D. H. Abbott, AlGaAs/GaAs cascade solar cell computer modeling under high solar concentration, *Solar Cells* **9** (1983) 311-326.
[195] M. F. Lamorte and D. H. Abbott, Influence of band gap on cascade solar cell efficiency, *Solar Cells* **10** (1983) 33-48.
[196] R. Radojcic, A. E. Hill and M. J. Hampshire, A numerical model of a graded band gap $CdS_xTe_{1-x}$ solar cell, *Solar Cells* **4** (1980) 109-120.
[197] D. Laser and A. J. Bard, Semiconductor electrodes: VII. Digital simulation of charge injection and the establishment of the space charge region in the absence and presence of surface states, *J. Electrochem. Soc.* **123** (1976) 1828-1832.



[198] D. Laser and A. J. Bard, Semiconductor electrodes: VIII. Digital simulation of open-circuit photopotentials, *J. Electrochem. Soc.* **123** (1976) 1833-1837.
[199] D. Laser and A. J. Bard, Semiconductor electrodes: IX. Digital simulation of the relaxation of photogenerated free carriers and photocurrents, *J. Electrochem. Soc.* **123** (1976) 1837-1842.
[200] D. Laser, Modes of charge transfer at an illuminated semiconductor electrode: A digital simulation, *J. Electrochem. Soc.* **126** (1979) 1011-1014.
[201] N. M. Bogatov, L. I. Gromovoi, M. B. Zaks, and E. V. Lelyukh, A numerical solution of the one-dimensional boundary value problem of charge transfer in solar cells, *Geliotekhnika* **18** (1982) 7-14.
[202] J. Newman, Numerical solution of coupled, ordinary differential equations, *Ind. Eng. Chem. Fund.* **7** (1968) 514-517.
[203] R. White, C. M. Mohr, Jr., P. Fedkiw, and J. Newman, The fluid motion generated by a rotating disk: A comparison of solution techniques, *Lawrence Berkeley Laboratory Report*, LBL-3910, November 1975.
[204] R. E. White, *Simultaneous reactions on a rotating-disk electrode*, Ph.D. thesis, University of California, Berkeley, March 1977, LBL-6094.
[205] D. J. Leary, J. O. Barnes, and A. G. Jordan, Calculation of carrier concentration in polycrystalline films as a function of surface acceptor state density: Application for ZnO gas sensors, *J. Electrochem. Soc.* **129** (1982) 1382-1386.
[206] J. A. Davis, R. O. James, and J. O. Leckie, Surface ionization and complexation at the oxide-water interface: I. Computation of electrical double layer properties in simple electrolytes, *J. Colloid Interface Sci.* **63** (1978) 480-499.
[207] J. A. Davis and J. O. Leckie, Surface ionization and complexation at the oxide-water interface: II. Surface properties of amorphous iron oxyhydroxide and adsorption of metal ions, *J. Colloid Interface Sci.* **67** (1978) 91-107.
[208] J. A. Davis and J. O. Leckie, Surface ionization and complexation at the oxide-water interface: 3. Adsorption of ions, *J. Colloid Interface Sci.* **74** (1980) 32-43.
[209] P. A. Iles, Evolution of silicon solar cell design, *9th IEEE Photovoltaic Specialists Conference*, Silver Springs, Maryland, 1972, pp. 1-5.
[210] B. Parkinson, An evaluation of various configurations for photoelectrochemical photovoltaic solar cells, *Solar Cells* **6** (1982) 177-189.
[211] M. E. Orazem and J. Newman, Mathematical modeling of liquid-junction photovoltaic cells: III. Optimization of cell configuration, *J. Electrochem. Soc.* **131** (1984) 2582-2589.
[212] R. N. Fleck, D. N. Hanson and C. W. Tobias, Numerical evaluation of current distribution in electrochemical systems, *Lawrence Berkeley Laboratory Report*, UCRL-11612, 1964.
[213] C. Kasper, The theory of the potential and the technical practice of electrodeposition: I. The general problem and the cases of uniform flow, *Trans. Electrochem. Soc.* **77** (1940) 353-363.
[214] C. Kasper, The theory of the potential and the technical practice of electrodeposition: II. Point-plane and line-plane systems, *Trans. Electrochem. Soc.* **77** (1940) 365-384.
[215] C. Kasper, The theory of the potential and the technical practice of electrodeposition: III. Linear polarization on some line-plane systems, *Trans. Electrochem. Soc.* **78** (1940) 131-146.
[216] C. Kasper, The theory of the potential and the technical practice of electrodeposition: IV. The flow between and to circular cylinders, *Trans. Electrochem. Soc.* **78** (1940) 147-161.

[217] C. Kasper, The theory of the potential and the technical practice of electrodeposition: V. The two-dimensional rectangular enclosures, *Trans. Electrochem. Soc.* **82** (1942) 153-185.
[218] H. F. Moulton, Current flow in rectangular conductors, *Proc. London Math. Soc. (Ser. 2)* **3** (1905) 104-110.
[219] J. Newman, The fundamental principles of current distribution in electrochemical cells, in *Electroanalytical Chemistry*, Ed. by A. J. Bard, Vol. 6 (1973), pp. 187-352.
[220] M. E. Orazem and J. Newman, Primary current distribution and resistance of a slotted-electrode cell, *J. Electrochem. Soc.* **131** (1984) 2857-2861.
[221] F. Bowman, *Introduction to Elliptic Functions with Applications*, Wiley, New York, 1953.
[222] M. Abramowitz and I. A. Stegun, *Handbook of Mathematical Functions*, Dover, New York, 1964.
[223] D. Canfield and S. R. Morrison, Electrochemical storage cell based on polycrystalline silicon, *Lawrence Berkeley Laboratory Report*, LBL-14639, 1982.
[224] N. Muller and D. Cahen, Photoelectrochemical solar cells: Temperature control by cell design and its effects on the performance of cadmium chalcogenide-polysulfide systems, *Solar Cells* **9** (1983) 229-245.
[225] N. L. Weaver, R. Singh, K. Rajeschwar, P. Singh, and J. DuBow, Economic analysis of photoelectrochemical cells, *Solar Cells* **3** (1981) 221-232.
[226] P. Singh and J. D Leslie, Economic requirements for new materials for solar photovoltaic cells, *Solar Energy* **24** (1980) 589-592.
[227] F. M. Kamel and A. Muhlbauer, Impact of solar cell efficiency on the design of photovoltaic systems, *Solar Cells* **11** (1984) 269-280.